UNIVERSITY OF CALIFORNIA SAN DIEGO

Accelerating and decelerating hippocampal theta oscillations via optogenetic stimulations has opposing effects on spatial working memory

A Thesis submitted in partial satisfaction of the requirements

for the degree Master of Science

in

Biology

by

Naomie Devico Marciano

Committee in charge:

Stefan Leutgeb, Chair
Ashley Juavinett
Jill Leutgeb

2020

The Thesis of Naomie Devico Marciano is approved, and it is acceptable in quality and form for publication on microfilm and electronically:

Chair

University of California San Diego

2020

DEDICATION

To my beloved grandparents, thank you for being an inspiration, and for the love and encouragement you have always given me.

To my parents, thank you for your continuous love and support. I would not be here if it wasn't for your sacrifices and for that I am eternally grateful.

To my brother, thank you for always pushing me to be a better person.

To Dan, thank for always believing in me and for never failing to provide reassuring advice.

TABLE OF CONTENTS

LIST OF ABBREVIATIONS

HC Hippocampus

mEC Medial Entorhinal Cortex

DG Dentate Gyrus

MSA Medial Septal Area

PV+ Parvalbumin

SWR Sharp Wave Ripple

LFP Local Field Potential

AAV Adeno Associated Virus

AP Anterior Posterior

ML Mediolateral

DV Dorsoventral

PFA 4% Paraformaldehyde

PBS Phosphate Buffered Saline

ChR2 Channelrhodopsin-2

eYFP Yellow Fluorescent Protein

mPFC Medial Prefrontal Cortex

LIST OF FIGURES

LIST OF TABLES

ACKNOWLEDGEMENTS

I would like to recognize Dr. Stefan Leutgeb for serving as the chair of my committee and the principal investigator for my project. In my time in the lab you have taught how to think like a scientist and have equipped me with the skills to become an independent researcher. Thank you for your continued support and mentorship.

I would also like to recognize Dr. Jill Leutgeb for her advice and guidance. Thank you for challenging me to ask difficult questions and for your valuable comments and feedback.

In addition, I would like to thank Dr. Ashley Juavinett for being part of my committee.

My committee members have served as ideal role models and taught me valuable lessons, which have helped me to become a better scientist. I know that this knowledge will continue to enhance my educational career, and I am thankful for that.

None of this would have been possible without the help of Maylin Fu through her service as a mentor during this project. Thank you for being patient with me as I learned, supportive when I struggled, and encouraging when I succeed.

I would like to thank Rachel Siretskiy and Marina Jaramillo for their indispensable help as well as Rina Patel with whom I've shared my master experience in the Leutgeb Lab. Thank you for your continued support and friendship.

Lastly, I would like to thank every member of the Leutgeb Labs for their continuous willingness to always help throughout every step of this project.

The data that are presented in this thesis were obtained in collaboration with Fu, Maylin L; Siretskiy, Rachel E; Jaramillo, Marina A; Leutgeb, Jill K; Leutgeb, Stefan. Naomie Devico Marciano was the primary author of this thesis.

VITA

2017-2018	Instructional Apprentice, Department of Biological Sciences, University of California San Diego
2019	Tutor, Department of Biological Sciences, University of California San Diego
2019	Bachelor of Science, University of California San Diego
2019-2020	Teaching Assistant, Department of Biological Sciences, University of California San Diego
2020	Teaching Assistant, Department of Psychology, University of California San Diego
2020	Master of Science, University of California San Diego

FIELD OF STUDY

Major Field: Biology

Studies in Neurobiology and Neurophysiology
Professors Jill Leutgeb and Stefan Leutgeb

ABSTRACT OF THE THESIS

Accelerating and decelerating hippocampal theta oscillations via optogenetic stimulations has opposing effects on spatial working memory

by

Naomie Devico Marciano

University of California San Diego, 2020

Professor Stefan Leutgeb, Chair

Brain oscillations are a key component of cognitive processing. It is believed that neural oscillations are an indicator of the timing of neuronal activity within and across different brain regions. Theta oscillations (7-9 Hz) are one of many brain rhythmic oscillations involved in information processing. In the rodent hippocampus, theta oscillations are generated by pacemaker GABAergic cells of the medial septal area and combine with local hippocampal computation to support cognitive functions. Previous studies have used optogenetic stimulations to entrain medial septum firing to accelerate hippocampal theta rhythm by 2 Hz or more above the endogenous range

to test the role of theta oscillations for cognitive function. These manipulations revealed that the acceleration resulted in memory impairment. However, it is unknown whether the impairment resulted simply from the disruption of an endogenous rhythm, or whether it is specific to these higher frequency stimulations. We used optogenetic techniques to target GABAergic parvalbumin cells in the mouse medial septal area to gain control of the theta rhythm. Using this technique, we entrained the hippocampal theta rhythm to frequencies both above and below the endogenous range. We found that a deceleration of the theta rhythm (to 4 and 6 Hz) did not cause an impairment of the hippocampal-memory task as observed with the accelerated rhythm (to 10 and 12 Hz). Therefore, we show that disruption of an endogenous oscillation does not necessarily result in an impairment of cognitive function. Our study further suggests that a deceleration of theta rhythm could result in an improvement of the hippocampus-dependent memory, and future studies could therefore address whether decelerated theta oscillations in the hippocampus facilitate the functional coupling of the hippocampus with other brain regions.

INTRODUCTION

Memory and the brain structures that support it

Evidence for the hippocampus' role in memory was initially identified when observing the amnesic behavior of patients such as Henry Molaison (H.M) (Squire, 2009). Patient H.M was the first and most famous amnesic patient, victim of uncontrollable epileptic seizures since the age of 10. In 1954, to control H. M's seizures, Dr. William Scoville performed a bilateral medial temporal lobectomy (Squire, 2009). The intervention included the removal of the hippocampi, parahippocampi and entorhinal cortices. Following this procedure, the neuropsychologist Brenda Milner observed that patient H.M had lost the ability to form new episodic memories – autobiographical and emotionally associated events (Penfield & Milner, 1958). However, his previously established long-term memories (such as childhood memories), personality, and motor skills, had not been damaged. These observations demonstrated that the hippocampus, and its surrounding cortical regions, played a critical role in the formation of declarative memories (Penfield & Milner, 1958).

The role of the hippocampus in the formation of declarative memories has since been confirmed with multiple animal studies (Korte & Schmitz, 2016). Studies done in monkeys demonstrated that damage to the medial temporal lobe resulted in memory impairment, specifically for spatial memory tasks (Mishkin, 1978). These studies were done to replicate the lesions sustained by H.M and reinforced the notion that particular types of memories are supported by structures of the medial temporal lobe. One such sub-category of memory is declarative memory which encompasses the facts (semantic) and events (episodic) we are able to consciously recall. The medial temporal lobe is made up of several structures that support cognitive and emotional

functions (Squire et al., 2004). These structures include the hippocampus, amygdala, the perirhinal, entorhinal, and parahippocampal cortices (Squire et al., 2004)

The hippocampus can be subdivided into several sub-structures: CA1, CA2, CA3 and dentate gyrus (Anand & Dhikav, 2012). The dentate gyrus receives input from layers II and III of the medial entorhinal cortex, these connections form the performant path (Green, 1964). Granule cells of the dentate send information to the pyramidal cells of the CA3 area, (Mossy Fiber pathway). The CA3 area in turn projects back onto itself (recurrent collaterals) and to the CA1 area (Shaffer collateral) (Green, 1964). Lastly, pyramidal cells of the CA1 area serve as the output for the hippocampus by sending their axons to the subiculum and the deeper layers of the medial entorhinal cortex (layer V & VI)(Andersen et al., 1971).

Brain oscillations that support memory

Each of the components of the hippocampus (Figure 1) generates a multitude of signals that can be recorded as different electrophysiological measurement. One of these measures are intracerebral local field potentials (LFP) which reflect the synchronous synaptic activity of neurons in the vicinity of the recording electrode (Denker et al., 2011).

LFP recordings allow researchers to identify different brain oscillations (Herreras, 2016). Brain oscillations, the rhythmic firing pattern of neurons, have been linked to cognitive processing in the healthy brain (Buzsáki & Draguhn, 2004). These oscillations are not only an indication of proper timing of neural activity or spiking, but they also indicate the coordination of activity across multiple brain regions (Fries, 2005). Furthermore, the disruption of these oscillations, such as a reduction in their amplitude, has been observed in numerous neurological diseases such as depression and Alzheimer's disease (Canali et al., 2015; Montez et al., 2009). Therefore, gaining

a better understanding of how these oscillations modulate neural functions could provide key insight for treatments that aim to improve cognitive functions including memory. For memory specifically, three distinct oscillations that can be recorded in the mouse hippocampus are thought to be particularly relevant. The three rhythms are Theta oscillations (7-9 Hz) (Colgin, 2016), Gamma oscillations (30-90 Hz) (Bragin et al., 1995), and Sharp Wave-Ripples (150-200 Hz) (Buzsáki et al., 2003; Buzsáki & Draguhn, 2004; Colgin, 2016). These oscillations have not only been reported in rodents, but have also been found in humans (Jiang et al., 2019; Lega et al., 2012).

Sharp Wave Ripples (SWRs), are composed of a coupled signal that consists of the sharp waves and a brief high frequency oscillation (i.e., ripple) (Colgin, 2016). The sharp waves are generated by excitatory synaptic inputs from the CA3 area to the CA1 area while ripples are locally generated in the CA1 area (Colgin, 2016). SWRs have been reported during slow-wave sleep, periods of immobility and reward consumption (Buzsáki, 1986) and have been linked to memory consolidation. SWR suppression following a hippocampal dependent memory task resulted in an impairment in task performance (Girardeau et al., 2009). SWRs are associated with the phenomenon of "replay" which refers to the reactivation of place cells' firing pattern that occurred during the exploration of an environment (Nádasdy et al., 1999). Ripples have therefore been linked to memory consolidation (Korte & Schmitz, 2016; Ólafsdóttir et al., 2018). Sharp Wave Ripples are events that can therefore be used as an indication that recording electrodes are in the hippocampal network.

Another of the mentioned hippocampal rhythms, Theta rhythm was first observed in rabbits (Green et al., 1960; Green & Arduinp, 1954), but has since been recorded in many other species including rodents, monkeys and humans (Buzsáki, 2002; Jacobs, 2014; Stewart & Fox, 1991). Local field potential (LFP) recordings have revealed that theta oscillations occur during periods of

movement as well as during REM sleep (Buzsáki, 2002; Vanderwolf, 1969). Moreover, theta oscillations have been linked to memory tasks and are believed to play an important role in the coordination of neural activity across different brain regions including the hippocampus, the prefrontal cortex and medial entorhinal cortex (G Buzsáki & Draguhn, 2004; Hasselmo, 2005).

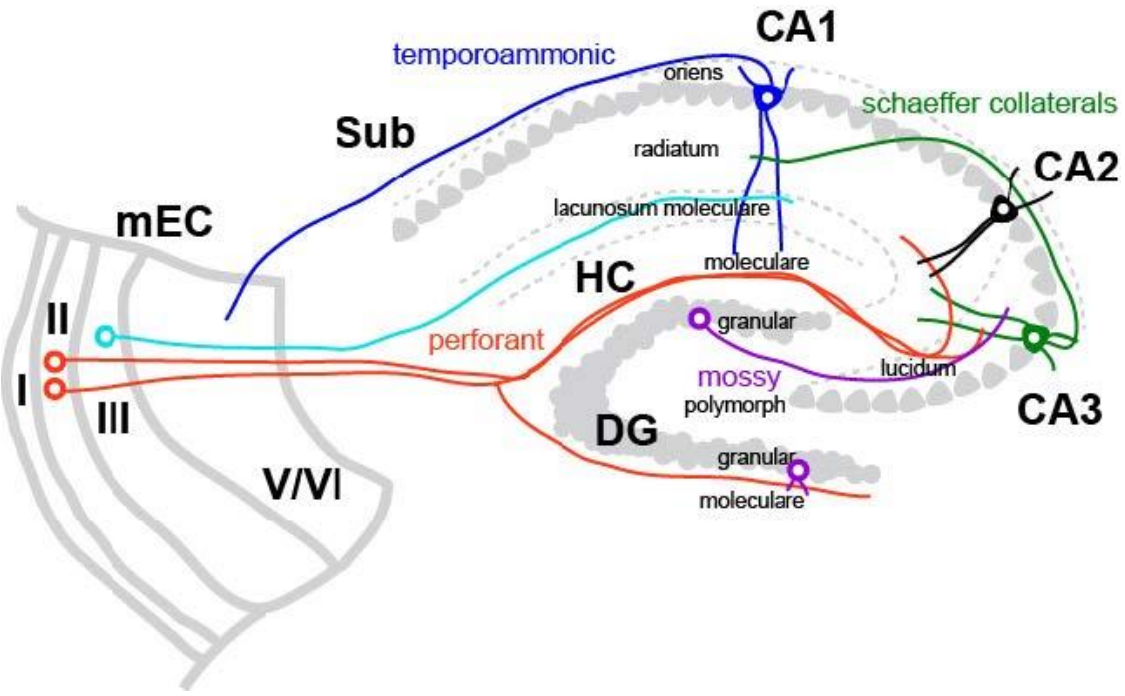

Figure 1. Anatomy of the Hippocampus and Medial Entorhinal Cortex (mEC).
Red, layer II mEC cells project to DG and CA3 via the perforant path. Light blue, layer III mEC cells project to CA1 pyramidal cells. Purple, DG cells project to CA3 via the mossy fiber pathway. Green, CA3 cells project to CA1 pyramidal cells via the Schaffer collaterals. Dark blue, CA1 pyramidal cells project to the subiculum and layers V and VI of the mEC via the temporoammonic pathway. From Quirk 2019, used with authorization.

Brain oscillations that support memory

It has been established that long-range projections from the medial septum area (MSA) support high amplitude theta oscillations in awake animals (Rawlins et al., 1979; Winson, 1978). The medial septal area is composed of the medial septum and the diagonal band nuclei (Freund, 1989). The medial septum receives projections from hippocampal interneurons and in turn sends

long-range projections to the hippocampus and the medial entorhinal cortex via the fornix. The medial septum is composed of GABAergic cells that express parvalbumin (PV) (Freund, 1989) and cholinergic cells. GABAergic cells send projections to the interneurons of the hippocampus and the medial entorhinal cortex (Freund & Antal, 1988; Gonzalez-Sulser et al., 2014) while cholinergic cells send projections to interneurons and principal cells of the hippocampus and the medial entorhinal cortex (Lewis & Shute, 1967). GABAergic PV cells of the medial septum fire at a specific rhythm, which is locked to the hippocampal theta frequency (Petsche et al., 1962). The firing of these cells has also been correlated to the running speed of the animal (Mcfarland et al., 1975). Medial septal lesions result in loss of hippocampal theta rhythm (Rawlins et al., 1979; Winson, 1978). These findings support the "pacemaker hypothesis", suggesting that GABAergic medial septum cells drive theta oscillations in the hippocampus

Disruption of the theta rhythm by lesions or by inactivation of the medial septum during hippocampus-dependent memory tasks proved to severely impair performance (Leutgeb & Mizumori, 1999; Winson, 1978). Although the inactivation of the medial septum resulted in decreased performance when performing a memory task (Morris Water Maze task), memory of the task could be restored by rhythmic theta stimulation at 7.7 Hz of the fornix (McNaughton et al., 2006; Shirvalkar et al., 2010). These findings support the functional role played by theta oscillation in memory.

Manipulating Theta oscillations in the hippocampus

Electrical stimulations have been used to manipulate oscillations in different behavioral tasks. The development of optogenetics has allowed researchers to more precisely generate activity in a defined neuron population (Boyden et al., 2005). By using channelrhodopsin-2 (ChR2), a light

sensitive sodium channel in combination with an optic fiber to deliver light to the targeted areas, it has been possible to modulate neural spiking with millisecond precision (Boyden *et al*., 2005). By shining blue light, it is possible to activate these sodium channels, causing an influx of sodium ions into the cells, which results in depolarization. When the depolarization reaches threshold, the neuron will generate an action potential and propagate the action potential down its axon (Boyden *et al*., 2005). Many have used this technique to either enhance, suppress or modify theta rhythm in the hippocampus to better understand how it regulates memory (Blumberg et al., 2016; Robinson et al., 2016; Vandecasteele et al., 2014; Zutshi et al., 2018). However, there have not been many studies which have combined spatial working memory tasks with optogenetics.

Particularly, the Leutgeb lab demonstrated that it was possible to modify theta frequency in the hippocampus of freely moving animals using optogenetics to stimulate the septal PV-positive cells of mice (Quirk et al., 2016; Zutshi et al., 2018). Shifting theta frequency by 2 Hz or more higher than the endogenous theta range (7-9 Hz) resulted in impairment of a spatial working memory task (Quirk et al., 2016). This impairment was comparable to that observed in rats with hippocampal lesions (Chenani et al., 2019). These findings provide evidence of the important role that normal theta oscillations can have for sustaining working memory. It is unknown however, to what extent these manipulations alter oscillatory patterns of neuronal cell populations and whether it is specifically an increase in the theta frequency that results in this impairment. To further identify the role of precise timing in neural networks, it is therefore of interest to determine whether slowing down theta rhythm in the hippocampus has the same consequences as accelerating theta oscillations.

In addition to the hippocampus, other brain regions are also modulated by theta oscillations. It has been reported that theta regulates the timing within the entire entorhino-hippocampal loop

and that it also coordinates the timing between prefrontal cortex and the hippocampus during memory tasks (Harris & Gordon, 2015; Siapas et al., 2005). Coordination across these brain regions is known to play a critical role in spatial working memory. However, we are now just starting to understand how information flows between them. It is therefore important to better understand the role that theta oscillation could play in modulating the activity across the hippocampus and prefrontal cortex and how the spiking of theta coordinates specific cognitive functions. Moreover, the prefrontal cortex displays an endogenous 4 Hz oscillation (Fujisawa & Buzsáki, 2011), and it is known that the prefrontal cortex is engaged during spatial working memory tasks in human and rodents (Riley & Constantinidis, 2016). However, the effects of a 4 Hz oscillation in the hippocampus has not yet been studied. It is therefore of interest to try to understand if slowing down the endogenous theta oscillations in the hippocampus could allow for an increase in coordination between the hippocampus and the prefrontal cortex. If this were the case, it would be relevant to understand what effects (if any) this would have and how this would contribute to working memory.

In this project, we aim to take advantage of the optogenetic stimulation model to gain access and to modulate the endogenous theta oscillation. By doing so, we expect to alter the neural spike timing without affecting other types of neuronal activity such as population sparsity. We hope to address what effects modulating hippocampal theta frequency can have on spatial memory. Specifically, we will focus not only on stimulating at frequencies above 8 Hz, but we will also conduct behavioral testing while stimulating at frequencies below 8 Hz. Our hypothesis builds on the previous results that shifting theta oscillation to 10 Hz or more causes memory impairments (Quirk et al., 2016). It is therefore possible that by changing theta oscillations to be 2 Hz or more below the endogenous range, similar impairments in spatial memory could arise. Alternatively, it

is also possible that a slower theta rhythm does not cause a deficit in performance. Lastly, it is possible that the slower theta rhythm results in an improvement of the performance of mice on the hippocampal-dependent spatial alternation task.

CHAPTER I- METHODS

Subjects:

All procedures used in this project were approved for use by the Institutional Animal Care and Use Committee (IACUC) at the University of California San Diego (UCSD). All experiments were conducted following the guidelines outlined by the National Institutes of Health for the care and use of laboratory animals.

We used genetically modified mice that selectively express CRE in parvalbumin neurons (129p2-Pvalbtm1(cre)arbr/j, Jackson Labs). The study's subjects were composed of 6 female (4 ChR2 , 2 controls) and 10 male (8 ChR2 , 2 controls) PV-Cre +/- mice. All animals were housed individually for at least a few days prior to starting any training or handling and throughout the experiment. They were kept on a 12-hour reverse light-dark cycle. Dark hours were from 8:00 am to 8:00 pm while light hours were from 8:00 pm to 8:00 am. During behavioral training and recordings, the animals were kept in a dark environment. The room was lit with dim light in one corner which served as an orienting landmark, and the environmental cues were kept stable. During the entirety of the behavior training and recording, animals were kept at approximately 85% of baseline body weight and were fed water *ad libitum.* This food restriction was necessary in order to ensure that the animals would eat the chocolate sprinkle reward delivered during the behavior task.

Behavioral training:

Apparatus:

The behavioral task was performed on a Figure-8 maze that was 50 cm above the ground with 75 cm long return and stem arms and 25 cm choice arms. Before placing an animal on the

Figure-8 maze, the maze was wiped with Clorox disinfecting wipes in order to remove the smell of any animal that was previously on the maze. This allowed the animals to feel more at ease on the maze.

Habituation:

Prior to the start of any behavioral training, the animals were brought to the experiment room in order to acclimate them to the novel environment. For about five days, the animals were handled for five to ten minutes by one of the personnel performing behavioral recordings, to allow them to become comfortable with researchers. A subset of the mice had their implant surgery prior habituation while the remaining mice had their surgery later during training. Delaying the surgery generally resulted in a better electrophysiological signal at the time of testing.

Training phases

Prior to behavioral training on each day, animals were weighed to assess their health.

Phase 0:

During this phase, the animals were placed on the Figure-8 maze for ten to fifteen minutes and allowed to freely explore the maze. Approximately 12 chocolate sprinkles were placed at several locations of the maze. Once animals were comfortable eating on the maze (eating at least 9/12 sprinkles), they were moved to phase 1.

Phase 1:

During this phase, the animals were placed on the Figure-8 maze and forced to alternate between left and right arms using cardboard barriers**.** Animals were forced to continuously alternate on the maze for 40 trials or 20 minutes, whichever occurred first. A chocolate sprinkle was placed at the reward location of each arm, and the consumption of the reward was monitored. Animals were not allowed to turn back or run past the central arm of the maze. Once the animal

could run in the forced alternation without being pushed and eating most rewards, they were moved to phase 2.

Phase 2:

During this phase, the animals were placed on the Figure-8 maze and tasked with alternating turns to the left and to the right arms of the maze in order to obtain a chocolate sprinkle (Figure 2). In this phase, the animals were no longer forced to pick between arms, rather they were expected to remember which arm they had run through in the previous lap and to pick the opposite arm on the subsequent lap in order to obtain a reward. Animals were to run 80 laps or for 40 minutes, whichever came first. Animals were still not allowed to turn around or run past the central arm. If the animal paused for longer than 10 seconds at any point, a light touch of the tail with a little noise was performed. The goal of the noise was to have classical conditioning of the tail touch and the noise in order to avoid touching the animal on subsequent training phases**,** otherwise contact between the animal and researcher was kept at a minimum. After successfully having 80% or greater accuracy on the 80 trials for 2 out of 3 consecutive days, animals that had not received the implant surgery prior to habituation were prepared for implant surgeries. Once they recovered from the implant surgery, they repeated phase 2 with the recording tether cable. After reaching 80% correct on 2 out of 3 consecutive days, animals were moved to phase 3. The animals that had received implant surgery prior to habituation repeated phase 2 with the tether cable as well before moving on to phase 3.

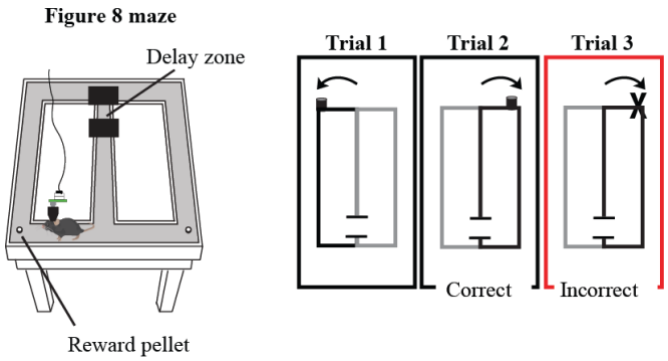

Figure 2. Figure-8 Spatial Working Memory Task.
Mice were trained to alternate between left and right arms of the maze to retrieve a chocolate reward. Animals were moved to the next phase of the experiment when they reached 80% accuracy or higher on 2 out of 3 consecutive days. In later phases of the task, 2s and 10s delays were introduced rendering the task hippocampus dependent.

Phase 3:

This phase was only performed with implanted animals. Similarly to phase 2, the animals were expected to alternate between arms of the maze in order to receive the chocolate sprinkle. Unlike phase 2, which is hippocampal-independent, this phase introduced a hippocampus-dependent spatial memory component. During each daily session, the animals alternated between 10 laps with no delay, 2-second delay or 10-second delay, and the sequence was repeated twice for a total of 60 trials. The delay was introduced at the beginning of the central arm using barriers that entrapped the animal. The order of the delay was pseudorandomized each day of the training, to ensure that the animal did not get used to a particular sequence of delays. In order to advance to the next step, animals needed to correctly perform the task with 80% or greater accuracy (over the 60 trials) and with a performance of at least 75% on the 10s delay trials.

Phase 4:

This phase includes optical stimulation and LFP recordings. Each day, the animal ran a total of 60 laps alternating between no delay, 2-second, and 10-second delay every 10 laps. Furthermore, rhythmically pulsating laser stimulation to the MSA was on during every other block

of 10 laps. Each day a different stimulation frequency was used. The order of stimulation blocks and delays was pseudo-randomized each day (Table 1).

If the recording for a day showed no endogenous theta oscillation, that specific stimulation day was re-run at the end of the 10 days of recording.

Table 1 **Example of randomization of the order of stimulation frequency and delays for recording days.**

	F10		F11	
Day	**Frequency**	**Delay**	**Frequency**	**Delay**
1	6 Hz	2s 10s 0s	10 Hz	2s 10s 0s
2	12 Hz	0s 2s 10s	12 Hz	10s 2s 0s
3	10 Hz	10s 2s 0s	6 Hz	0s 2s 10s
4	4 Hz	10s 0s 2s	8 Hz	10s 0s 2s
5	8 Hz	0s 10s 2s	4 Hz	0s 10s 2s
6	10 Hz	2s 0s 10s	6 Hz	2s 0s 10s
7	6 Hz	10s 2s 0s	8 Hz	0s 2s 10s
8	8 Hz	2s 0s 10s	12 Hz	2s 10s 0s
9	4 Hz	0s 2s 10s	4 Hz	10s 2s 0s
10	12 Hz	10s 0s 2s	10 Hz	10s 0s 2s

Surgeries

Surgical procedures were either performed before habituation (9 mice, viral vector surgery and implant surgery) or before habituation (7 mice, viral vector surgery) and in phase 2 (implant surgery). All surgeries were done following aseptic procedures. Animals were anesthetized in a chamber filled with 3.0% isoflurane at 1L Oxygen / min then moved to a stereotaxic frame (David Kopf Instruments, Model 1900) fitted with a nose cone. Isoflurane was initially administered at a

concentration of 2.5% isoflurane at 0.4L Oxygen / min and the concentration was adjusted based on the duration of the surgeries and weight of the animals. During all surgeries, the animals were kept on a heating pad at 37˚C. An ophthalmic lubricant ointment was applied to the animals' eyes to prevent dryness during the surgery.

Viral vector surgery

Parvalbumin(PV)-Cre mice aged 2 to 6 months were injected with cre-dependent viral vectors (AAV.EF1.DIO.ChR2.eYFP or AAV.EF1.DIO.eGFP) in order to express either channelrhodopsin (ChR2) or, for the control animals, a green fluorescent protein (GFP) in the MSA. Viral vectors were provided by Dr. Lim's laboratory (University of California, San Diego).

The fur near the skull of the animal was shaved off and the scalp was cleaned and disinfected with saline and antiseptic povidone-iodine solution. Once disinfected, the scalp was retracted using a midline incision, the animals were given a subcutaneous injection of 0.1 ml of 2% lidocaine as a local anesthetic. The skull was then leveled using bregma and lambda, great care was taken to ensure that the skull was also leveled along both the anterior-posterior and dorsal-lateral axis. Once aligned, a hole was drilled over the MSA to make a small craniotomy (+ 1.0 mm A/P; -0.7 mm M/L) and 1200 nl of the chosen virus was injected at a rate of 100 nl/min at three depths (400 nl at +1.0 mm A/P; -0.7 mm M/L, -4.8 mm DV; 400 nl at +1.0 mm A/P; -0.7 mm M/L, -4.6 mm DV; 400 nl at 1.0 mm A/P; -0.7 mm M/L, -4.2 mm D/V). The virus was delivered through a glass pipette using a micro syringe pump (Micro4, UMP3 UltraMicroPump, World Precision Instruments). The pipette was left in place for 5 minutes after the injection and then slowly retracted. The animals were subcutaneously injected with 0.05 mg / kg of 0.2% buprenorphine hydrochloride about 20 minutes before the end of surgery to act as a painkiller.

Mice were then sutured and placed back in their heated (37˚C) home cages until they successfully woke up from surgery. The animals were allowed to recover for a minimum of 5 days.

Microdrive and Optic fiber implant

The fur near the skull was again shaved off and the scalp was cleaned and disinfected with saline and antiseptic povidone-iodine solution. The scalp was retracted, and the skull was leveled between bregma and lambda.

Next, five holes were drilled in the skull in order to attach anchor screws and dental cement to secure the implant. A hole was drilled over the MS (+1 mm A/P, -0.7 mm M/L, -3.5 mm D/V) and the optic fiber was implanted at a 10˚ medial-lateral angle. A ground-screw was placed over the cortex. Next, a craniotomy was performed above the hippocampus (-1.9 mm A/P, +1.8 mm M/L, at a 3˚ anterior-posterior angle), and the dura was removed. A drive was positioned above this hole, and the tetrodes were lowered to 0.35-0.6 mm below the surface of the brain in the dorsal-ventral axis. Neuroseal (2 drops of Na_2 Alginate, 1 drop $CaCl_2$) was added to secure the drive into position. Several layers of dental cement were applied to further secure the drive and the screws. The animals were again injected with 0.05 mg/kg of 0.2% buprenorphine hydrochloride to act as a painkiller about 20 minutes before the end of the surgery. Mice were placed back into their heated (37˚C) home cage and allowed to wake up from surgery. Postoperative care was administered as needed for at least 5 days after surgery, until the animals fully recovered.

Recording protocol

Once animals had fully recovered from the implant surgery, they were brought back into the behavior room in order to be re-habituated.

The animals were then allowed to begin training or repeat phase 2 of the behavior in order to re-introduce the task and to allow them to adjust to running the behavioral task while wearing the implanted microdrive. Before every recording session, the tether cable was untangled and of proper length (not too tight nor too loose) to facilitate the animal's running. The first days, the maze was slightly moved to adjust for how the mice now ran with the cable as it could often bias one of the sides. Once a location was identified for which the mouse could alternate comfortably, the position of the maze was marked on the floor. Every behavioral day, the animal would run with the maze in its adjusted position.

While the animals were trained to run with the cable, the tetrodes of each microdrive were progressively lowered until the recording tetrodes reached the CA1 cell layer of the hippocampus. The turning of the electrodes was limited to 3/4 turns (339 μm) per day, but normally would be turned in increments of 1/8 (57 μm) to 1/4 (113 μm). By progressively lowering the electrodes we were able to properly time the training of the animal with the cable to the time when the cell layer was reached. The arrival to the cell layer was marked by the presence of SWRs detected in the LFP as well as by an increase of the theta amplitude.

Once the tetrodes had reached the cell layer and the animal had completed phase 3 of the training, the recording protocol began (Figure 3). The stimulation frequency and the order of delays followed the randomization explained in "Behavior phase 4".

Prior to starting any of the recordings, all channels of the microdrive were referenced to the quietest channels (usually one without cells) to subtract out baseline neuronal activity. This allows for better separation of cells during cell clustering analysis. Before running the spatial alternation task, a 10-15 minutes rest recording was performed, some animals were active during these recordings and these periods would therefore not be considered as rest for analysis. After

running the 60 laps of the spatial alternation task a second rest recording was performed. While the animal ran the task, both the LFP and the single cell spiking activity were recorded. A camera positioned at the ceiling allowed us to track the position of the animal using LED units connected to the microdrive.

During the recording days, the tetrodes were lowered slowly to allow us to record from different locations of the cell layer. If all 10 days of behavior showed good endogenous theta and the presence of pacing, the animal was sacrificed for histological analysis.

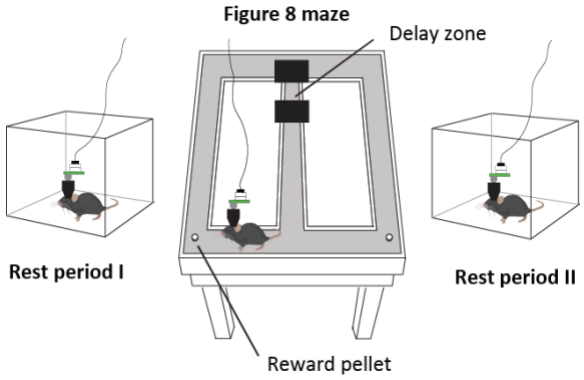

Figure 3. Spatial Working Memory Recording Paradigm.
Each spatial alternation task was preceded and followed by a 10-15 minutes "rest" period. The duration of the rest period depended on the activity level of the mouse and the presence of cells during the recordings. Shorter rest periods were recorded for more active mice or if no cells were present.

Electrophysiology recordings in freely moving mice

The microdrive assemblies implanted onto the brain of the mice facilitated the recording of Local Field Potential (LFP) and single-unit spiking. Electrode tips were plated with platinum to reduce the electrical impedances to between 150-250 kΩ at 1 kH**.** A preamplifier, tether and 16 channel acquisition system (Neuralynx, Inc.) was used to record and collect all the data for this experiment. LFP was sampled at 32,000 Hz and filtered between 1 and 1,000 Hz.

Laser stimulation

Light was delivered to the MSA using a 473 nm wavelength Blue DPSS Laser System though an optic fiber patch cord (Doric Lenses, MFP_200/240/1100-0.22_10m_FC-ZF1.25(F), 200 μm core, 0.22 NA) to the custom optic fiber implant. The optic fiber implant was made using an optic fiber (200 μm core, ThorLabs, 0.50 NA multimode fiber) that was glued to a zirconia ferrule (Precision Fiber Products, 230 μm). The optic fiber was sanded down to allow for maximum light through the fiber and cut to a length of 4-4.5 mm. The laser output intensity was adjusted to between 9.0 and 12.0 mW. Light was delivered at a 50% duty cycle at frequencies of 4, 6, 8, 10 and 12 Hz.

Perfusion and Histological procedures

After all recordings were done, the food deprivation of the animal was lifted. After a few days, mice were anesthetized in a chamber filled with 5% isoflurane. A lethal injection of Sodium Pentobarbital (240 mg/kg) was then given to the animals. The perfusion procedure began once the animals were confirmed to be unresponsive to a toe pinch. The animals were perfused with a saline solution (0.9%) for approximately 3 minutes, followed by ~50 ml of 4% Paraformaldehyde (PFA). Once the perfusion was completed, the animal's head was separated from the body and allowed to rest for about 1 hour to allow the PFA to continue to fix the brain tissue. This allowed for the tetrodes tracks to become better defined in the hippocampal region. The tetrodes were then slowly moved up and the brain extracted from the skull. The brain was refrigerated in 4% PFA for 24 hours and then moved to a 1X PBS solution until ready to section.

The MSA and hippocampus of the animals were sectioned using a vibratome. Coronal slices were cut every 40 μm. The slices were directly mounted as they were being cut.

MSA slices were cover slipped with DAPI solution (4′,6-Diamidino-2′-phenylindole dihydrochloride) and the hippocampal slices were stained using cresyl violet.

Quantification of viral vector expression and optic fiber placement

Sections of the MSA of the mice injected with the cre-dependent viral vector (AAV.EF1.DIO.ChR2.eYFP) were imaged using a virtual slide microscope (Olympus, VS120) at a 10x magnification using the same laser power and exposure time. For each animal, five sections (0.2 mm apart) along the antero-posterior extent of the MSA were chosen and analyzed using Fiji ImageJ. Three regions of interest (ROI) were determined. The first ROI was drawn around the medial septum, and two other ROI were drawn around the diagonal band of Broca in each hemisphere. The area of virus expression was calculated by subtracting the background from each image and measuring the area of opsin expression above a threshold of 0. The volume of opsin expression was then calculated by averaging the area of expression across the five sections per animal and multiplying by the distance between the sections.

In addition, the depth at which the optic fiber was implanted was determined from a section that displayed the trace of the tip of the optic fiber canula by measuring the distance from the top of the cortex to the tip of the cannula.

Statistical Analysis

All statistical analysis was performed using GraphPad Prism (version 8). Only recording sessions for which pacing was detected were used for the analysis. Unless a session was excluded, all animals have 2 recording sessions in which the same stimulation frequency was used, therefore the behavior of the animal was averaged across these two sessions for the analysis.

We used a T-test to evaluate the differences in performance for each stimulation frequency and delay type when the light was turned on and when it was turned off. The obtained p values were corrected using a Holm-Bonferroni correction to account for the multiple comparisons.

CHAPTER II – RESULTS

Histology confirmed recording site and viral vector expression

To examine the contribution of theta frequency to hippocampus-dependent memory, we modified theta frequency and tested behavioral performance of mice on a hippocampal dependent task. Using a method that was shown to be effective in previous studies (Quirk et al., 2016; Zutshi et al., 2018), theta frequency was modified by optogenetically stimulating PV neurons in the medial septal area. To selectively express the Cre-dependent viral vector in PV-positive neurons of the medial septum, we used PV-Cre mice. An adeno-associated viral vector (AAV) was used to express channelrhodopsin-2 (ChR2) in these neurons (Figure 4A), rendering them responsive to blue light stimulation. These GABAergic septal cells send long-range projections to the inhibitory interneurons of the hippocampus and are thought to coordinate hippocampal oscillations through these projections (Figure 4B). The delivery of blue light with the optic fiber placed in the medial septum area (MSA) activates the GABAergic cells expressing the ChR2 construct, which allowed us to modulate the hippocampal theta oscillation to the desired frequency.

Recording electrodes placed in the hippocampus allowed us to monitor the cell spiking activity as well as the LFP (Figure 4C). The presence of sharp wave ripples (SWRs) was used as an indication that the recording electrodes were correctly lowered to the hippocampus during in vivo recordings. By performing histological analysis of the animal's hippocampus, we were able to confirm the presence of tetrode tracks in the targeted CA1 region**,** which indicated that our recording electrodes had correctly reached the cell layer **(**Figure 4C).

The histological analysis of the MSA revealed the expression of the AAV vector as it was coupled with a yellow fluorescent protein (eYFP) (Figure 4D).

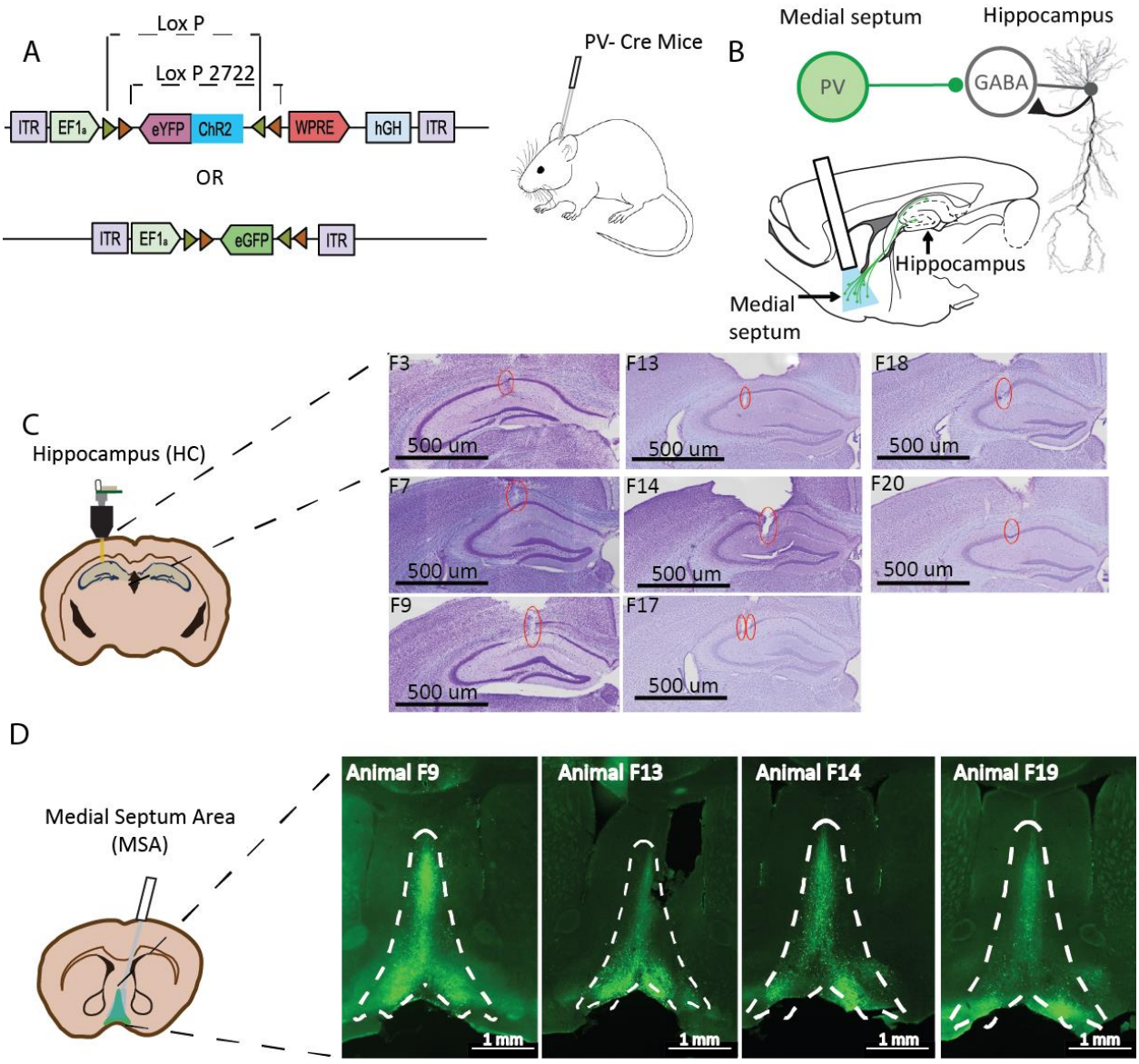

Figure 4. Histology analysis confirming viral expression in the MSA and tetrode location in the HC. (A) Schematic representation of the AAV vectors used to express either ChR2 (top) or GFP (bottom) in PV-Cre transgenic mice. (B) Schematic of optogenetic stimulation of MSA PV cells expressing ChR2 projecting to HC interneurons. (C, left) Recording electrodes were lowered to the CA1 area of the HC. (C, right) example histology of the HC shows the location of the tetrodes tracks (red circles). (D, left) Optic fiber placed above the MSA. (D, right) Example histology of the MSA demonstrates how expression can be quantified using the green fluorescence co-expressed with the opsin viral vector.

The efficiency of pacing was assessed by determining whether oscillation frequency was modified

We performed rhythmic optogenetic stimulations of the PV neurons of the MSA using frequencies below the endogenous theta range (4 and 6 Hz), at the endogenous range (8 Hz) and above the endogenous range (10 and 12 Hz).

During each day of the behavior recording phase, one of 5 stimulation frequencies was used for an animal (see Methods for details). The mice began by running the alternation task without stimulation (Figure 5A), and their behavioral performance was recorded. After 10 laps the laser was turned on, and the animal completed the next 10 laps with stimulation. Blocks without and with stimulation alternated and each of the three delay conditions was repeated once, which yielded a total of 60 laps in 6 blocks (Figure 5B). A time-frequency spectrogram of the LFP was generated to illustrate the power spectra over the entire recording session. As expected, the LFP frequency changed when the optical stimulation was turned on and returned to the endogenous oscillation frequency when it was turned off. Turning on the stimulation resulted in an immediate change of the hippocampal oscillation to the stimulated frequency (Figure 5B). Once the stimulation was turned off, hippocampal oscillation returned to the endogenous theta range. Furthermore, there was an increase in the power during the stimulation compared to when the stimulation was off (in the example, from $2x10^8$ to $6x10^8$). We were able to measure the how reliably the LFP was altered by calculating, for every 2 s period, the peak LFP oscillation frequency and by comparing the distribution of the peak frequencies between the period when the stimulation was turned on with the period when it was off (Figure 5C). Turning on the stimulation also caused the amplitude of the LFP oscillation to change compared to the amplitude of the endogenous oscillations (Figure 5D).

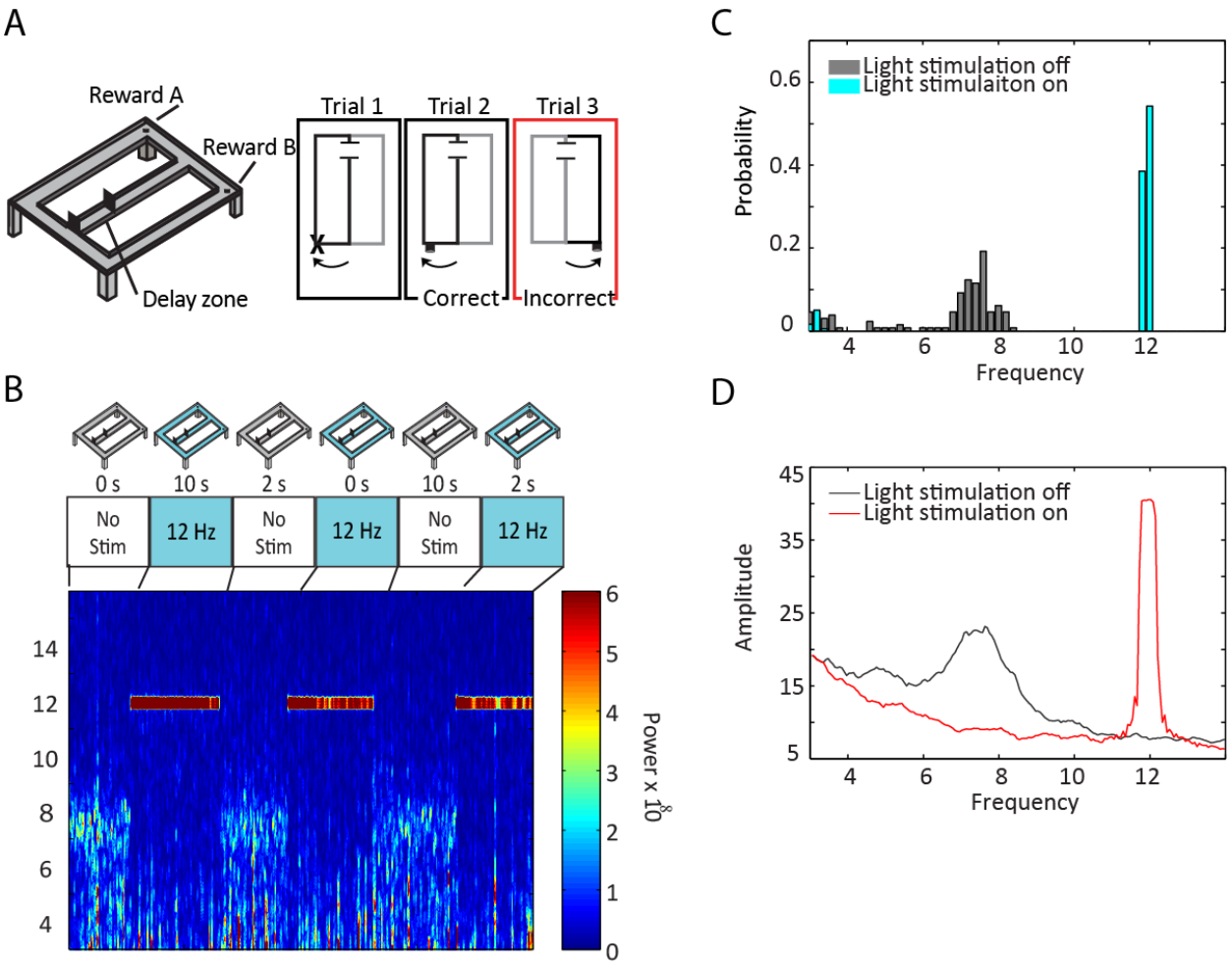

Figure 5. Optogenetic stimulation of MSA PV neurons controlled the LFP oscillation in the HC while the mice ran the alternation task.

(A) ChR2 and control animals were trained on a spatial alternation task with either no delay or delays of 2s or 10s. (B) The animal's performance was tested in alternating blocks with and without stimulation. One stimulation frequency was used per day with different stimulation frequencies (4, 6, 8, 10 or 12Hz) used each day. Example session with 12 Hz stimulation shown with the order of delays and alternating blocks with the stimulation on or off. A time-frequency spectrogram of the LFP shows that during stimulation the LFP oscillation frequency changes to match the stimulation frequency and replaces the endogenous theta oscillation. Endogenous theta oscillations returned immediately after the stimulation was turned off. (C) Histograms showing the probability density function of the peak frequency when the laser stimulation is off (grey) and when it is turned on at 12Hz (cyan) (D) Spectrogram of the LFP amplitude when the stimulation is off (grey) and when it is turned on (red).

Changes in LFP oscillation frequencies indicated that hippocampal oscillations were paced by septal stimulation

To test whether we were able to alter the frequency of the hippocampal theta oscillation, we analyzed the changes in hippocampal local field potentials (LFP). In examples of successful pacing (Figure 6) we were able to observe that the oscillation frequency changed from ~7 Hz when the stimulation is off (Figure 6A) to 12 Hz when it is turned on (Figure 6B). We measured the shift in frequency using three different scores. For each score, we compared the predominant oscillation frequency during the no delay/no stimulation block with the predominant oscillation frequency during the no delay/stimulation block of each recording session (see Figure 6C and D for details about each of the calculations). We selected the no delay trials in the behavioral task for this analysis because electrical noise can be created in the delay zone during delay trials when the mouse's recording implant contacts the cardboard stoppers. Because the 4 tetrodes that were implanted in the hippocampus were of slightly different length and we were not able to move them independently, it was usually the case that the tetrodes were not at the same depth within the hippocampus. The amplitude of theta oscillations varies dependent on the depth in hippocampus, and there was therefore variation in theta amplitude across recording channels (i.e., one channel per tetrode). We reasoned that the channel with the highest endogenous theta amplitude would allow for the best assessment of the effect of the pacing and therefore selected the pacing score from the channel with the most prominent endogenous theta oscillation. Because the three scores were based on different calculations, the endogenous theta amplitudes during no stimulation blocks were also calculated in three different ways. It is therefore possible that the channel that was selected for reporting differed between the three pacing scores.

The analysis of the probability distribution-based pacing scores contributed to determine a pacing score threshold of 0.5 for the selection of a recording session. If the pacing score was below 0.5, the recording session and the behavior associated with it were excluded from the analysis.

Figure 6. A shift of the LFP frequency from the endogenous frequency to the stimulation frequency indicates successful pacing.

(A) LFP trace with the light stimulation off, filtered signal (3-20 Hz, red), unfiltered (black). (B) LFP trace with the light stimulation on, laser light stimulation (blue), filtered signal (3-20 Hz, red), and unfiltered signal (black). (C, right) Histograms showing the probability density function of the peak LFP frequency when laser stimulation is off (grey) and when it is on at 12 Hz (cyan). The signal on 4 recording electrodes is shown (channel 1-4). (C, left) Amplitude of the LFP oscillations when the stimulation is off (grey) and when it is on (red). (D) Table depicting the 3 pacing scores and the 3baseline measurements obtained from the pacing algorithm. Scores: (1) Probability distribution-based score: Peak probability in the stimulation range (± 1 Hz) during stimulation/ Peak probability in the endogenous range (7- 9 Hz) during no stimulation. (2) Maximum amplitude-based score: Maximum LFP amplitude near the stimulation frequency during stimulation / maximum LFP amplitude in the endogenous theta range during no stimulation. (3) Mean amplitude-based score: Mean amplitude near stimulation frequency during stimulation / mean amplitude in the endogenous theta range during no stimulation. Baseline measurements: Peak base = peak probability in the endogenous range during no stimulation. Max base = maximum LFP amplitude in the endogenous theta range during no stimulation. Mean base = mean LFP amplitude in the endogenous theta range during no stimulation.

A

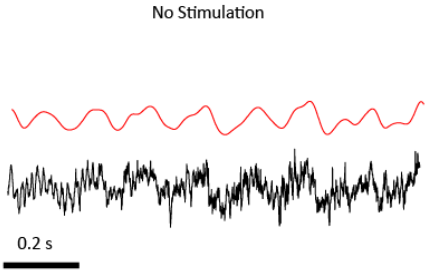

B

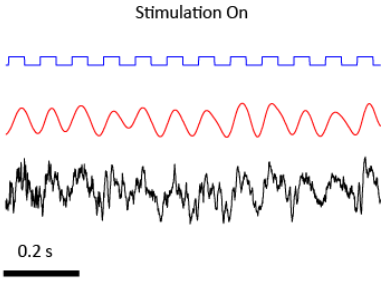

C

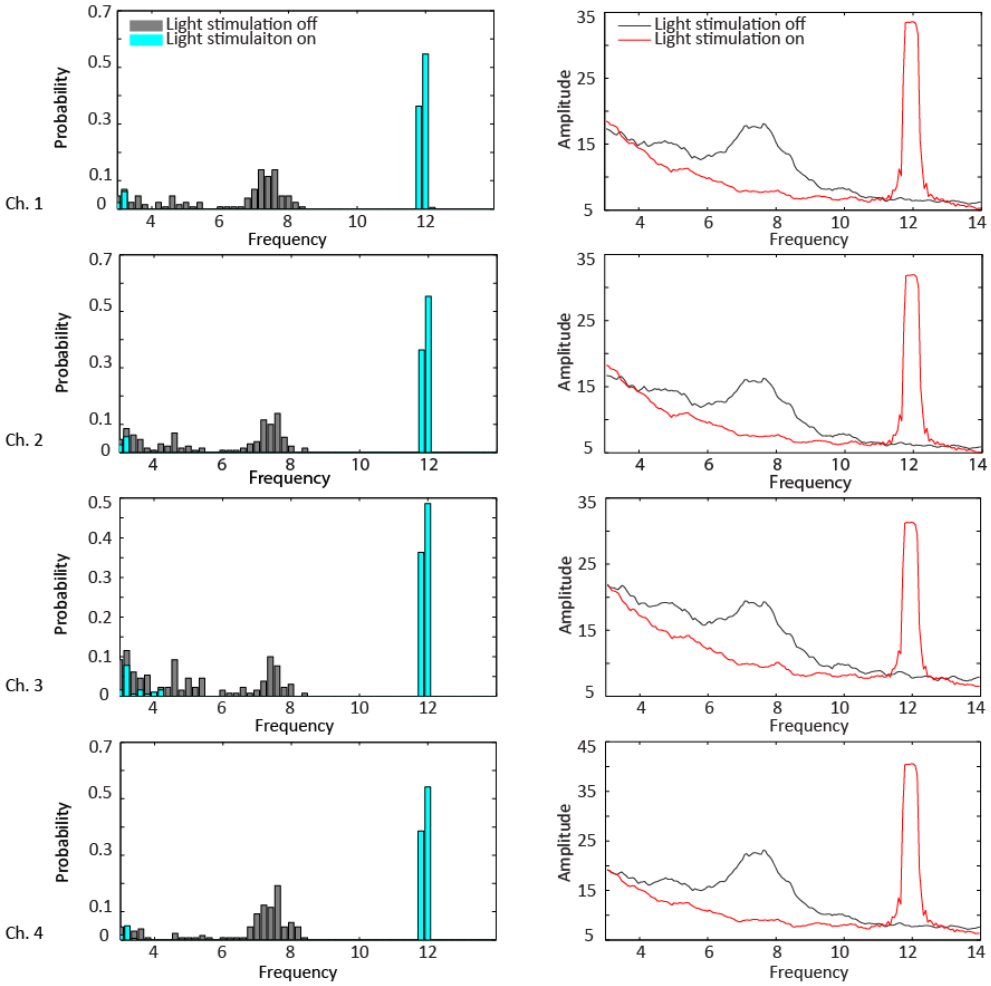

D

	Channel 1	Channel 2	Channel 3	Channel 4
Probability distribution-based score	3.9540	3.9944	4.8603	2.8179
Maximum amplitude-based score	1.8543	1.9620	1.6116	1.7526
Mean amplitude-based score	0.9505	0.9973	0.8851	0.9115
Peak probability of endogenous oscillation	0.1385	0.1385	0.1000	0.1923
Maximum endogenous theta amplitude	18.1212	16.2669	19.4465	23.1416
Mean endogenous theta amplitude	14.8177	13.4493	16.1460	18.6284

Pacing at frequencies below 8 Hz resulted in harmonics

During the lower frequency stimulations, it was possible to detect the presence of harmonics. These manifest as oscillations at an integral multiple of the stimulation frequency. For 4 Hz stimulations, harmonics could be detected at 8 Hz (2nd harmonic) and 12 Hz (3rd harmonic) (Figure 7B). To obtain a 4 Hz stimulation, the blue laser light pulses 4 times per second. For a 4 Hz oscillation to occur, an oscillation needs to happen with every pulse of light. In the example shown, we could detect 2 or 3 oscillation happening for every light cycle. The oscillation peaks are highlighted by blue arrows (2 peaks per light cycle) or green arrows (3 peaks per light cycle) and indicate that during the 4 Hz stimulation harmonic oscillations were occurring. When two oscillations per light cycle occurred, this resulted in an 8 Hz harmonic, and when three oscillations per light cycle occurred, this resulted in a 12 Hz harmonic. In some instances, the harmonics were more prominent and thus had a higher amplitude than the stimulation frequency itself (Figure 7C). In these cases, we therefore calculated the pacing score using the frequency of the harmonic rather than the stimulation frequency. The channel with the best endogenous theta oscillation was selected and the pacing score for the harmonic with the highest amplitude was calculated. For example, during a 4 Hz session, the 8 Hz harmonic was more prominent than oscillations at the simulation frequency (Figure 7 D). Therefore, the reported pacing score was for the harmonic at 8 Hz (0.68) rather than the base frequency at the 4 Hz stimulation (0.21). It is evident that the 8Hz oscillation detected in these recordings is due to a harmonic and not due to a persistence of the endogenous theta because a narrow amplitude peak is detected precisely at 8 Hz rather than the broad distribution that is typical for the endogenous signal (grey line).

Figure 7. Example of a pacing score that was higher at a harmonic than at the base frequency.
(A-B) LFP traces when the stimulation is off or on, filtered signal (3-20 Hz, red), unfiltered (black), laser stimulation (blue) (B) Arrows point to peaks corresponding to a 12 Hz harmonic (blue) or to an 8 Hz harmonic (green). (C) Histograms showing the probability density function of the predominant LFP frequency in each 2 s interval when the laser stimulation is off (grey) and when it is turned on at 4 Hz (cyan) for channel 1 calculated with expected peaks at 4 Hz, 8 Hz and 12 Hz (from left to right). (D) LFP amplitude when the stimulation is off (grey) or when it is on (red). During stimulation, multiple peaks are observed in the signal from channel 2. (E) Table depicting the 3 pacing scores and the 3 baseline values obtained from the pacing algorithm. The pacing score was calculated using either the base frequency or harmonics as the reference frequencies (4, 8 and 12 Hz). Channel 1 was selected for having the best endogenous theta oscillation for the probability distribution based-score, and channel 2 was selected for the amplitude-based scores.

A

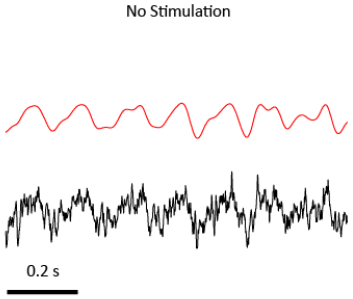

B

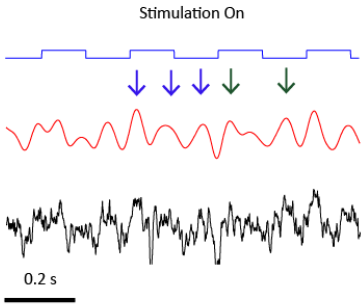

C

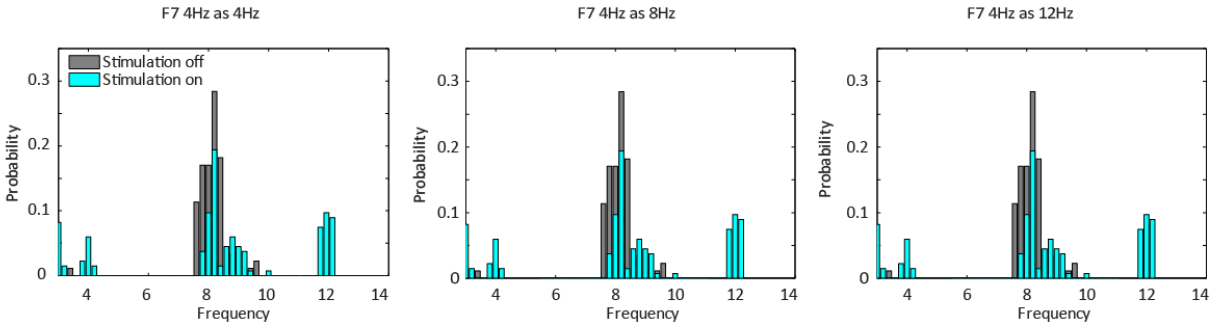

D

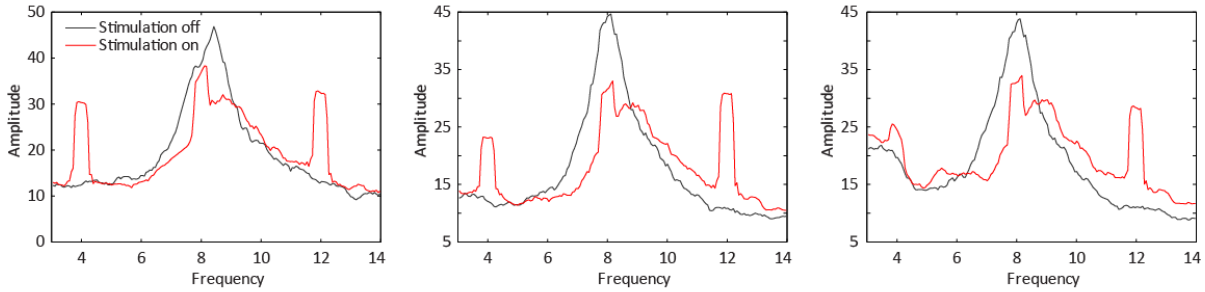

E

	as 4 Hz	as 8 Hz	as 12 Hz
Probability distribution-based score (Ch 1)	0.2101	0.6829	0.3414
Maximum amplitude-based score (Ch 2)	0.5201	0.7387	0.6915
Mean amplitude-based score (Ch 2)	0.4518	0.7258	0.5285
Peak probability of endogenous oscillation	0.2840	0.2840	0.2840
Maximum endogenous theta amplitude	44.67442	44.67442	44.67442
Mean endogenous theta amplitude	34.4134	34.4134	34.4134

Effects of light delivery to the MSA of control animals

Lastly, we needed to address the possible effects of shining a blue light onto the MSA of the mice. To do this, we injected mice with a viral vector containing a Green Fluorescent Protein (GFP) (Figure 4A). In these animals, a comparison of the LFP signal between periods when the 12 Hz light stimulation was either on or off had no apparent effect on the hippocampal oscillation (Figure 8A and B). The probability distributions and amplitudes during periods with and without stimulation therefore overlapped (Figure8C) and the lack of oscillations at the pacing frequency resulted in pacing scores close to 0 across all channels (Figure 8D).

Figure 8. Control animals showed no pacing when the stimulation was turned on.
(A-B) LFP traces with and without 12 Hz stimulation, respectively. Filtered LFP signal (3-20 Hz, red), unfiltered LFP signal (black), laser stimulation (blue). (C, right) Histograms showing the probability density function of the predominant LFP oscillation when the laser stimulation is off (grey) and when it is on at 12 Hz (cyan). The distributions do not differ for each of the 4 recording electrodes (channel 1-4). (C, left) No change in the amplitude of the LFP when the stimulation is off (grey) and when it is turned on (red). (D) Table depicting the 3 pacing scores and the 3 baseline values obtained from the pacing algorithm.

A

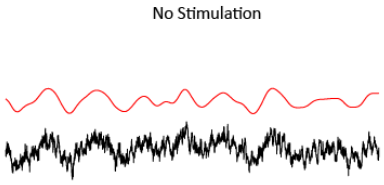

B

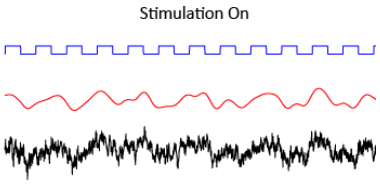

C

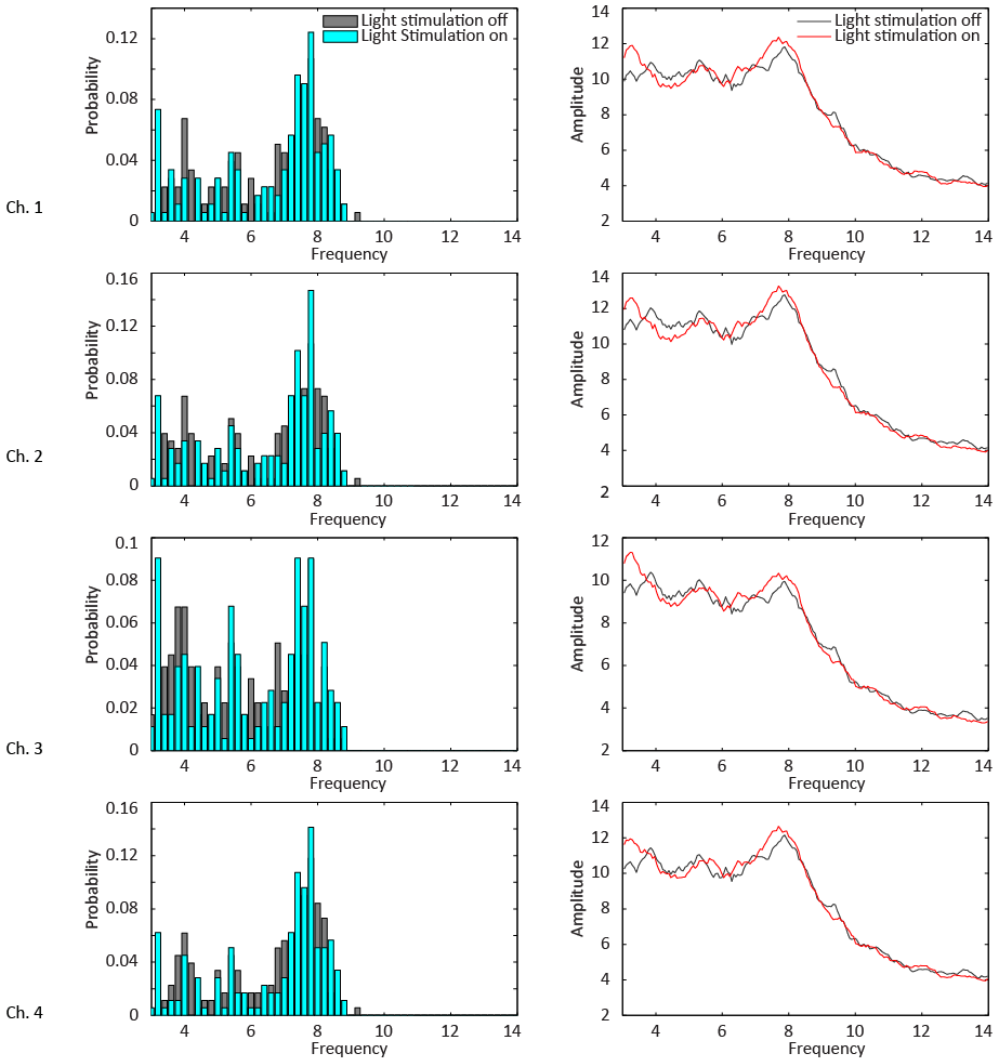

D

	Channel 1	Channel 2	Channel 3	Channel 4
Probability distribution-based score	0	0	0	0
Maximum amplitude-based score	0.4238	0.4020	0.4244	0.4199
Mean amplitude-based score	0.4394	0.4127	0.4394	0.4311
Peak probability of endogenous oscillation	0.1067	0.1067	0.0899	0.1180
Maximum endogenous theta amplitude	11.8268	12.766	9.9511	12.1544
Mean endogenous theta amplitude	10.4358	11.2530	8.8365	10.7459

Changes in performance were measured to determine if changing hippocampal theta oscillations affected non-hippocampal dependent memory

Although the following figures are separated based on the type of delay, all delays were run each day by the animals. As described in the methods, animals ran in blocks of 10 trials with different delays (no delay, 2s delay, and 10s delay) and with the stimulation either on or off on alternating blocks, which resulted in a total of 60 trials. Each animal performed the task for 10 days of recordings, with each one of the five stimulation frequencies on two of the testing days. The performance of each animal in the different conditions was averaged across the two days with the same stimulation frequency. Delays are depicted separately for analysis purposes.

We used two tests for normality, the D'Agostino and Pearson test and the Shapiro test. The Shapiro test did not identify any differences from normality and, using a D'Agostino and Pearson test, only data for the no delay 10 Hz and the no delay 12 Hz conditions were not normally distributed. Because the no delay condition does not belong to the hippocampal-dependent memory conditions that our hypothesis focuses on, we proceeded with parametric testing for the behavioral analysis. Furthermore, because of the small sample size of the control group (n = 4), normality could also not be tested using the D'Agostino and Pearson test. All data was normally distributed if tested using a Shapiro test.

During the continuous version of the task (no delay), the percent correct choice of mice with ChR2 expression did not differ between stimulation and no stimulation blocks (t-test: 4 Hz, n = 11, p = 0.86; 6 Hz, n = 12, p = 0.90; 8 Hz, n = 12, p = 0.14; 10 Hz, n = 11, p = 1; 12 Hz, n = 11, p = 0.66). The same conclusion can be reached for the performance of the control animals (n = 4 for all frequencies, t-test: 4 Hz, p = 0.30; 6 Hz, p = 0.55; 8 Hz, p = 0.07; 10 Hz, p = 0.70; 12 Hz, p = 0.50) (Figure 9A). Because our experimental design included stimulation blocks and no

stimulation blocks on each test day, the statistical testing was performed using the pairwise difference between blocks when the stimulation was turned on and when the stimulation was turned off (Figure 9B). Positive values indicate better task performance when the stimulation was on, and negative values indicate a worse task performance when the stimulation was turned on. For ChR2 animals across all frequencies, the mean change in performance was between -4.6 % and 1.4 %, for the control animals the mean change in performance was between -10.0 % and 7.5 %. Taken together, none of the stimulating frequencies which modulated hippocampal theta oscillations resulted in a change in the memory performance of mice in the non-hippocampal dependent alternation task.

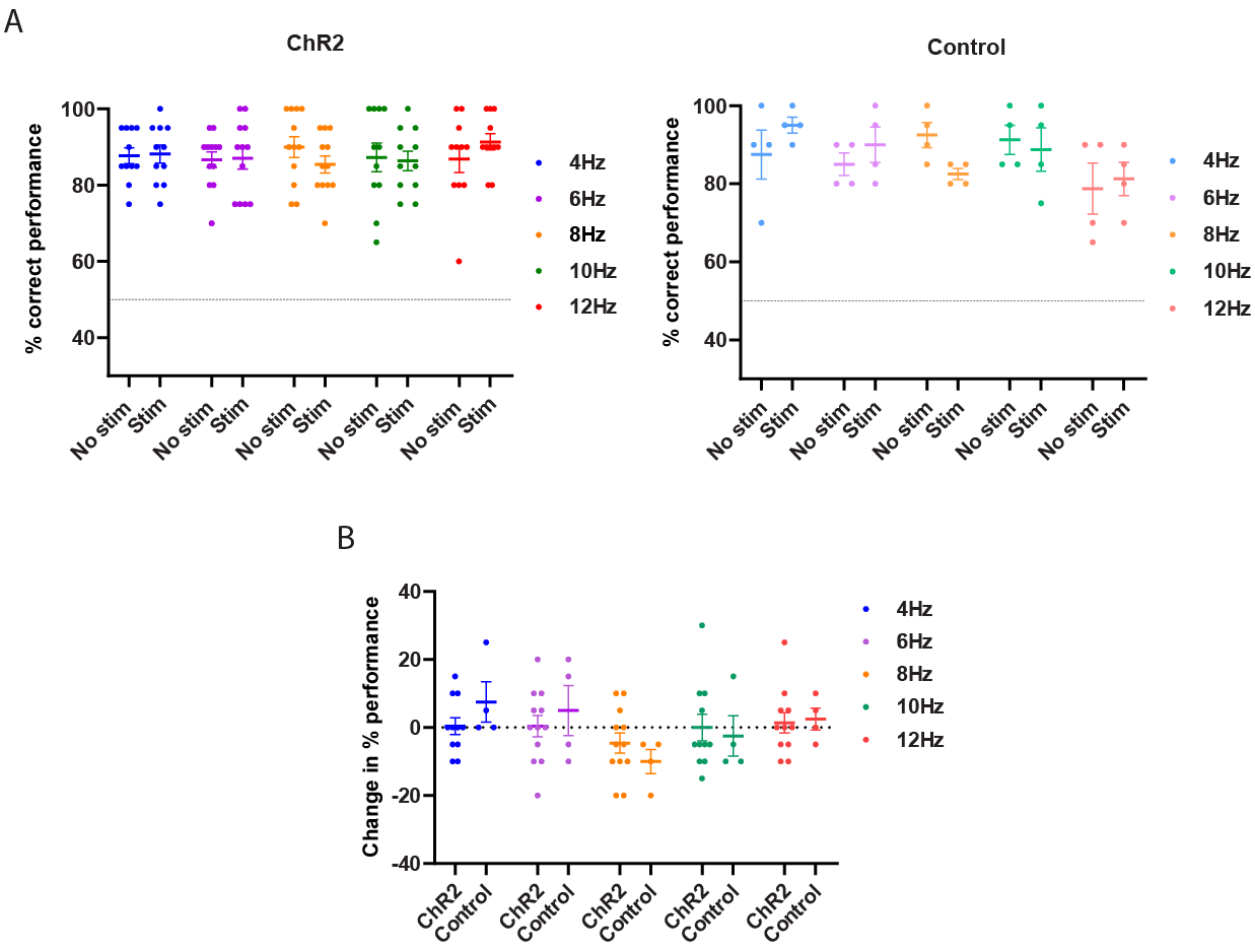

Figure 9. Modulating theta oscillation in the HC did not cause a change in the performance of mice on the continuous, non-hippocampal dependent, alternation task.
(A) Percent correct choices of mice when performing the alternation task with and without optical stimulation. Each dot represents the averaged performance of one mouse across the two days with the same stimulation frequency (ChR2 animals, left, n=12 for 6 and 8Hz and n=11 for 4, 10 and 12 Hz; controls, right, n=4). (B) Change in percent correct performance = Percent correct performance with stimulation on – Percent correct performance with stimulation off. Positive values indicate better performance when stimulation is on, negative values indicate worse performance when stimulation is on (see text for statistics).

Changes in performance were measured on a 2s delay version of the alternation task to determine the effect of modulating theta oscillations in a hippocampal dependent task

To analyze the effect of modulating theta oscillations in the hippocampus, we used a hippocampus dependent version of the alternation task by introducing delays on the stem of the maze. By introducing a delay, we were able to make the spatial alternation task rely on long term

memory which depends on the hippocampus (Ainge et al., 2007). All the data for the 2s delay condition is normally distributed, and statistical analysis was performed using a parametric t-test.

The percent correct choices of mice with ChR2 expression between blocks when the stimulation was either on or off did not differ for any of the stimulation frequencies (4 Hz, n= 11, $p = 0.47$; 6 Hz, n = 12, $p = 0.80$; 8 Hz, n = 2, $p = 0.47$; 10 Hz, n = 11, $p = 0.10$; 12 Hz, n = 11, $p = 0.76$). This was also the case for control animals (n = 4 for all frequencies, 4 Hz, $p = 0.55$; 6 Hz, $p = 0.06$; 8 Hz, $p = 0.85$; 10 Hz, $p = 0.09$; 12 Hz, $p = 0.22$) (Figure 10A). The change in performance was calculated as previously described. The mean performance across all stimulation frequencies varied between -8.6 % and 1.7 % for animals with ChR2 expression and between -7.5 % and 7.5 % for control animals (Figure 10B).

Taken together, accelerating or decelerating theta oscillations in the hippocampus had no effect on the mice's performance in the spatial alternation task with a 2s delay.

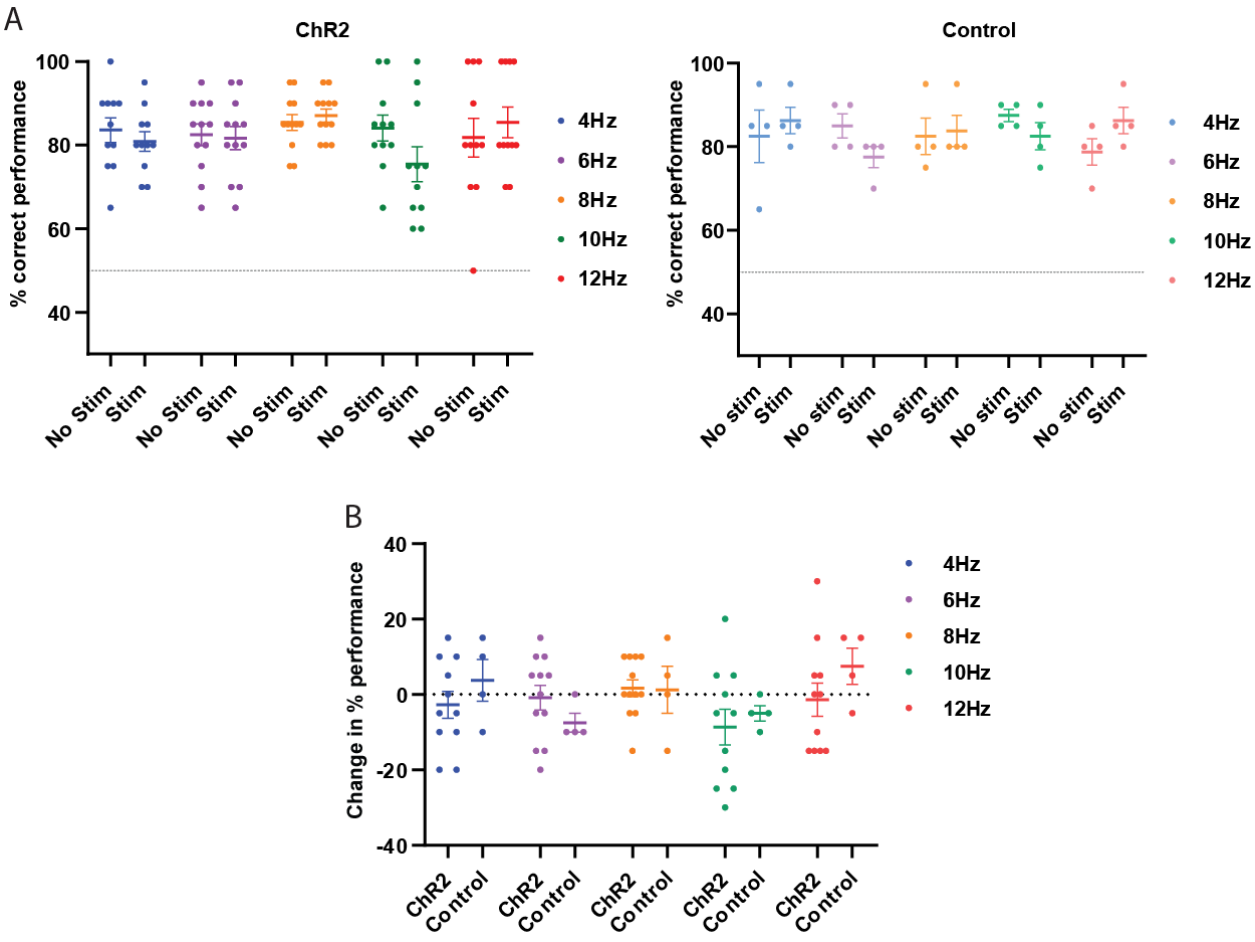

Figure 10. Modulating theta oscillation in the HC did not cause a change in the memory performance of mice on the hippocampus dependent version of the alternation task with a 2s delay.
(A) Percent correct of the mice when performing the alternation task with and without optical stimulation. Each dot represents the averaged performance of one mouse across the two days with the same stimulation frequency (ChR2 mice, left, n = 12 for 6 and 8 Hz and n = 11 for 4, 10 and 12 Hz; controls, right, n = 4). (B) Change in percent correct performance= Percent correct performance with stimulation on – Percent correct performance with stimulation off. Positive values indicate better performance when stimulation is on, negative values indicate worse performance when stimulation is on. (see text for statistics)

Changes in performance were measured on a 10s delay version of the alternation task to determine the effect of modulating theta oscillations in a hippocampal dependent task

In the 10s delay condition, similarly to the 2s delay condition, the animals were delayed this time using two cardboard blockers to prevent them from turning back. Here, trends in the effect of theta pacing on the memory performance of the mice became apparent. With one of the stimulation frequencies below the endogenous range, the percent correct choices of the mice with ChR2 expression were higher during blocks with stimulation on compared to blocks with stimulation off (t-test: 4 Hz n = 11 p = 0.02). Conversely, with one of the stimulation frequencies above endogenous range stimulation, the percent correct choices decreased during blocks with the stimulation on (t-test: 12 Hz n = 11 p = 0.04) (Figure 11A). With the 6 Hz, 8 Hz, and 10 Hz stimulation frequencies, no change in performance could be detected (t-test: 6 Hz, n = 12, p = 0.2; 8 Hz, n = 12, p = .90; 10 Hz, n=11, p=0.44). Changes in behavioral performance were not observed in the control group (n= 4 for all frequencies 4 Hz p = 0.83, 6 Hz p = 0.91, 8 Hz p = 0.23, 10 Hz p = 1, 12 Hz p = 0.20) .

When looking at the calculated change in performance, the trend became more apparent with stimulation frequencies below the endogenous range resulting in positive values (% change in performance: 4 Hz, n = 11, 8.64%; 6 Hz, n = 12, 4.18%) and stimulation above the endogenous range resulting in negative values (% change in performance: 10 Hz, n = 11, -4.55; 12 Hz, n = 11, -7.73%) (Figure 11B). As previously mentioned, positive changes indicate an improvement in performance when the stimulation is turned on, and negative changes indicate an impairment. The change in performance was lowest in the 8 Hz stimulation frequency (n= 12, 0.42%) , which falls within the endogenous theta range. A similar trend cannot be identified in the control animals (%

change in performance n = 4 for all frequencies: 4 Hz, 1.25%; 6 Hz, -1.25%; 8 Hz, 6.25%; 10 Hz 0.0%; 12 Hz, -11.25%) (Figure 11B).

While significance was reached for two of the stimulation frequencies with the t-test, the experimental design required that statistical tests be performed for each of the 5 stimulation frequencies. It is therefore necessary perform a correction for multiple comparisons. After applying a Holm-Bonferroni correction, the significance threshold becomes $\alpha = 0.01$ for the first p-value, however our lowest p value is for 4 Hz at $0.02 > 0.01$ which indicates that none of our differences were significant after correction.

To summarize all the analysis of the behavioral performance on the alternation task, after correction for multiple comparison none of the differences obtained were statistically different. As seen in Table 2, only in the 10s delay condition with 4 or 12 Hz stimulations did the performance of the ChR2 mice on the spatial alternation task differ significantly between blocks with the stimulation on or stimulation off ($p < 0.05$). When accounting for the multiple comparisons across frequencies for each delay, the differences are no longer significant.
In the control group, none of the changes in performance detected were different (Table 3).

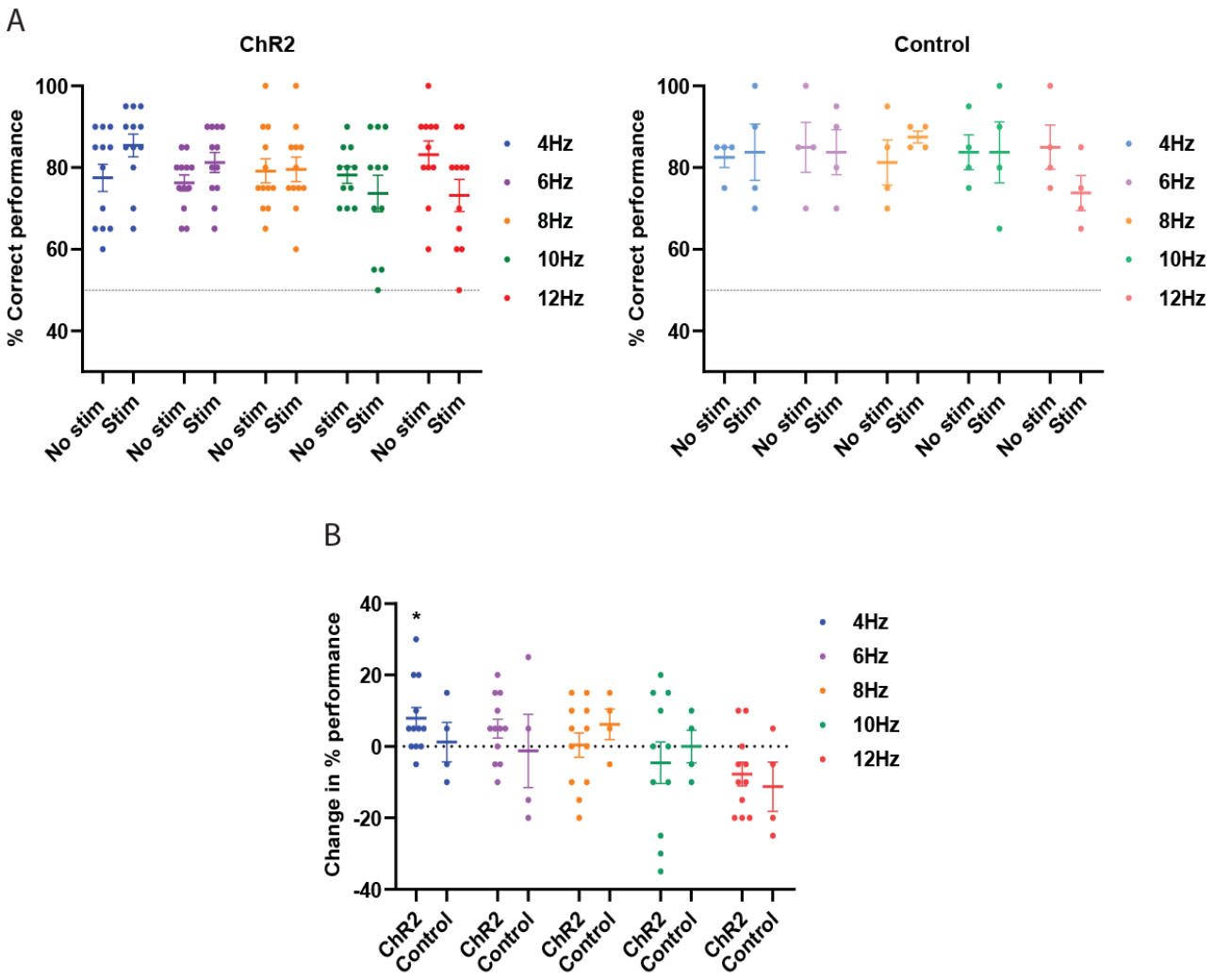

Figure 11. In the 10s delay version of the spatial alternation task, trends for an improved memory performance with 4 Hz stimulation and for an impaired memory performance with 12 Hz stimulation were observed.

(A) Percent correct choices of mice that performed the alternation task with and without optical stimulation. Each dot represents the averaged performance of one mouse across the two days when the same stimulation frequency was used (ChR2 animals, left, n=12 for 6 and 8Hz and n=11 for 4, 10 and 12 Hz; controls, right, n=4). (B) Change in percent correct performance = Percent correct performance with stimulation on – Percent correct performance with stimulation off. Positive values indicate better performance when stimulation is on, negative values indicate worse performance when stimulation is on. (see text for statistics).

Table 2 Statistical Analysis of ChR2 animals' performance across frequencies and delays

Delay	Paired t- test, p values					Holm-Bonferroni correction
	4 Hz n = 11	6 Hz n = 12	8 Hz n = 12	10 Hz n = 11	12 Hz n = 11	
No delay	0.86	0.90	0.14	1	0.66	N.S
2s	0.47	0.80	0.47	0.10	0.76	N.S
10s	0.02	0.21	0.90	0.45	0.04	N.S

Table 3 Statistical analysis of control animals' performance across frequencies and delays

Delay	Paired t- test, p values					Holm-Bonferroni correction
	4 Hz n = 4	6 Hz n = 4	8 Hz n = 4	10 Hz n = 4	12 Hz n = 4	
No delay	0.30	0.55	0.07	0.70	0.50	N.S
2s	0.54	0.06	0.85	0.10	0.22	N.S
10s	0.83	0.91	0.24	1	0.20	N.S

Pacing efficiency's effect on behavior

To address the question of whether the strength of the pacing influenced the behavioral performance, we analyzed the relationship between these two variables (Figure 12). For each stimulation frequency, the change in performance in each individual delay (no delay, 2 or 10s) was plotted as a function of the pacing score selected for that day. In this analysis, the behavior was not averaged across each animal as the pacing score could vary between sessions. A simple linear regression analysis showed that the slopes are not different from 0, indicating that there was no specific relationship between the strength of the pacing and the behavioral outcome as seen in Figure 12A.

To investigate whether the viral expression could affect our pacing abilities, we quantified the volume of eYFP expression in the MSA. The viral vector used to express ChR2 is coupled with a yellow fluorescence protein (eYFP) which allowed us to observe the extent of viral expression in PV+ cells in the MSA. We found that there was no linear relationship nor correlation between the total volume of viral expression and the probability distribution-based pacing score (Figure 12B).

Figure 12Strength of pacing does not correlate with performance on the alternation task nor with volume of viral vector expression in MSA.
(A-E, left) Scatterplots of the pacing score versus the change in Percent correct choices on the alternation task by the stimulation. None of the slopes are significantly different from 0. (A-E, right) Scatterplots of volume of eYFP expression in the MSA and averaged pacing efficiency per frequency across all animals.

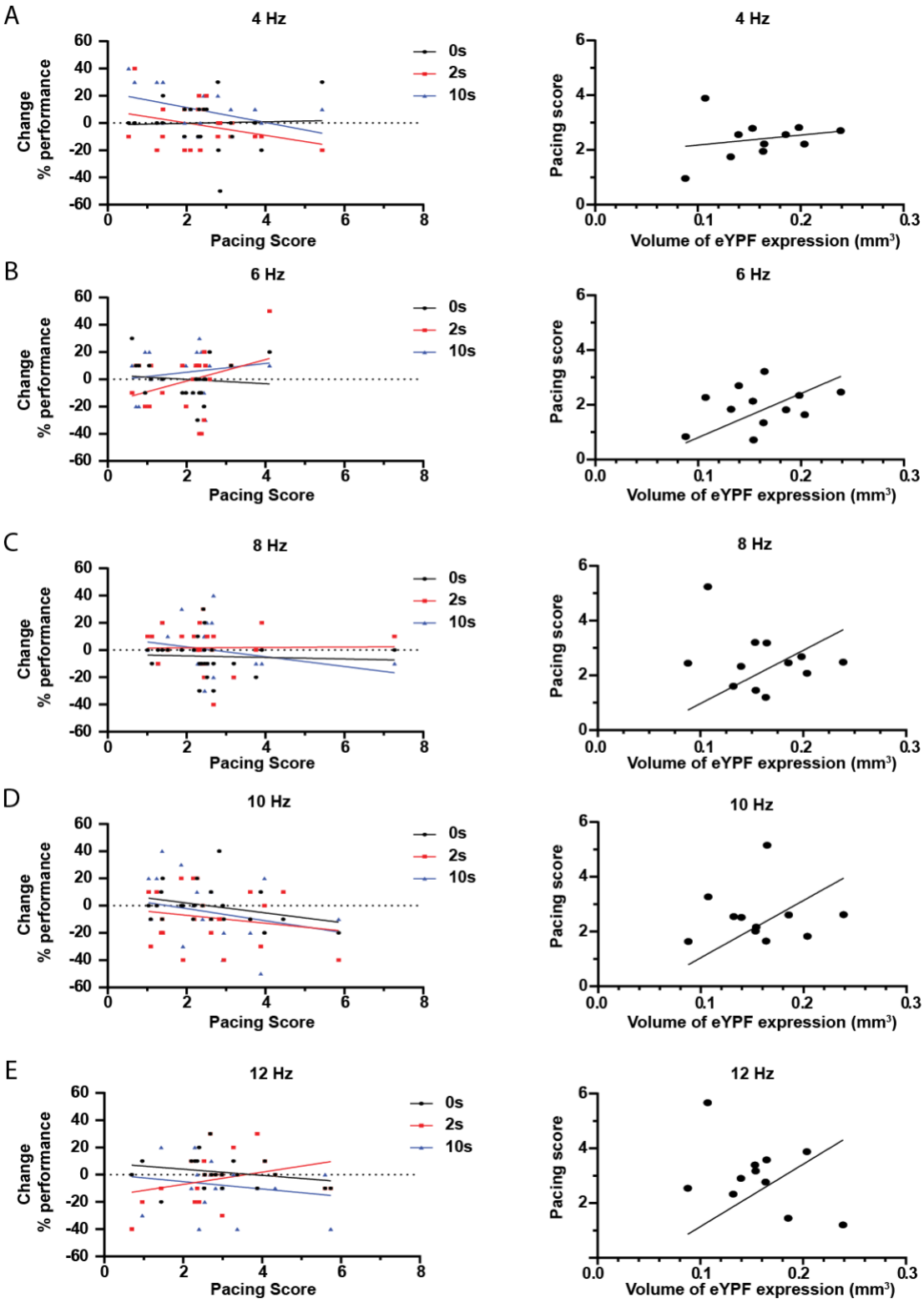
A
4 Hz
Change % performance
Pacing Score
0s
2s
10s
Pacing score
Volume of eYPF expression (mm³)
B
6 Hz
C
8 Hz
D
10 Hz
E
12 Hz

CHAPTER III- DISCUSSION

Theta oscillations are a prominent rhythm found in the hippocampus of mammals and rodents during periods of movement and REM sleep (Buzsáki, 2002; Jiang et al., 2019; Lega et al., 2012; Vanderwolf, 1969). Studies have demonstrated that hippocampal place cells, which are a component of spatial navigation, fire at a specific time in the theta cycle, a phenomenon known as phase precession (Buzsáki & Moser, 2013; O'Keefe & Recce, 1993). Other studies have abolished or reduced theta oscillations in the hippocampus and have found that it resulted in an impairment in spatial memory (Hasselmo, 2005; Winson, 1978). These findings taken together point to the critical role of hippocampal theta oscillations in memory encoding and retrieval. The evidence that theta oscillations are controlled by the pacemaker cells in the MSA, and that optogenetic pacing of these PV neurons can supersede the endogenous theta oscillations provides a unique opportunity to study the effects of modulating theta oscillations (Gogolák et al., 1968; Hangya et al., 2009; Petsche et al., 1962; Shirvalkar et al., 2010; Zutshi et al., 2018). Here we showed that rhythmic optogenetic stimulation of septal PV cells did not only effectively increase the oscillation frequency in the hippocampus (Zutshi et al., 2018; Quirk et al., 2016) but that it could also decrease the oscillation frequency. Using this method, we therefore tested the effects on spatial working memory while decelerating the theta rhythm to frequencies of 4 Hz and 6 Hz, as well as while accelerating the theta rhythm to frequencies of 10 Hz and 12 Hz. In agreement with a previous study done in our lab, we found that increasing the theta oscillation frequency to 12 Hz points to an impairment in spatial working memory. Most strikingly, our data provides preliminary evidence that decreasing the hippocampal theta oscillation to 4 Hz could result in an improvement of spatial working memory.

Extensive research has been done on the genesis of hippocampal theta oscillations. Based on the findings that about half of septal projections are cholinergic and that half are GABAergic and that septal lesions substantially reduced hippocampal theta, the generation of theta oscillations was initially attributed to both cholinergic and GABAergic neurons of the MSA (King et al., 1998; Kramis et al., 1975). To address this, Yoder and Pang preceded to selectively lesion cholinergic or GABAergic septal cells and found that hippocampal theta during locomotion was more strongly attributed to GABAergic neurons (Yoder & Pang, 2005). Specifically, combined lesions of GABAergic MSA neurons and EC inputs to the hippocampus were needed to fully eliminate hippocampal theta oscillations during locomotion. The disruption of the cholinergic input combined with EC lesion resulted in a decrease of hippocampal theta amplitude but did not eliminate the oscillations during locomotion (Yoder & Pang, 2005). Therefore, the rhythmic firing of GABAergic neurons and more pronounced effects of selective lesions of GABAergic neurons on theta oscillations, suggest a more direct role of the GABAergic cells for generating theta oscillations, in particular in periods of movement (Freund & Antal, 1988; Gonzalez-Sulser et al., 2014; Vandecasteele et al., 2014; Yoder & Pang, 2005; Zutshi et al., 2018). Furthermore, it has previously been reported that optogenetic activation of MSA PV+ cells allows to precisely control the hippocampal theta oscillations frequency (Bender et al., 2015; Fuhrmann et al., 2015; Zutshi et al., 2018), while a similar effect was not observed with stimulation of cholinergic cells (Vandecasteele et al., 2014). Our study therefore utilizes the optogenetic control of PV+ cells to modulate hippocampal theta oscillations to specific frequencies.

In order to analyze the efficiency of pacing at the various stimulation frequencies, we needed to quantify how the LFP could be modulated. Three metrics were designed to allow us to quantify

the effects of our manipulation, we refer to these metrics as pacing scores. The pacing scores allowed us to estimate the extent of the change in LFP frequency by comparing whether oscillations at the endogenous frequency or at the stimulation frequency are more prominent. However, during 8 Hz stimulation, these methods are more challenging to apply because the peak of the stimulation frequency overlaps with the peak of the endogenous theta oscillation frequency (7-9 Hz). However, with an 8 Hz stimulation frequency, the maximum and the mean amplitudes of the LFP narrowed at the stimulation frequency, which results in a narrow and large peak at 8 Hz whereas the endogenous amplitudes were more distributed along the 7 -9 Hz range (Figure 7). The pacing scores, in particular the ones that are based on the frequency distribution and on the peak amplitude, are therefore also high when 8 Hz stimulation successfully paces oscillations.

Previous studies had focused on the ability to increase theta oscillations by optogenetic stimulations to the MSA. Here we also tested the effect of a decrease in the theta frequency on hippocampus-dependent behavior. In our attempts to pace hippocampal theta oscillations to frequencies below the endogenous theta range, we noted the emergence of harmonics. Several theories exist which would argue that the harmonics detected in the frequency domain of the LFP are artifacts. For instance, when applying a Fourier transforms to represent a wave in the frequency domain, the sharp edge of the sawtooth wave results in harmonics. It has therefore been suggested that the detection of harmonics could be an artifact caused by the asymmetric sawtooth shape of theta oscillations (Cole & Voytek, 2016). However, here we show by examining the raw signals, that we were able to detect distinct additional waves within each light stimulation cycle during the 4 Hz stimulation, which strongly suggests that our harmonics did not merely result from an asymmetry in the paced oscillations (Figure 7B). While harmonics therefore appear to be a genuine

consequence of low frequency stimulation, the emergence of the harmonics poses challenges when quantifying the pacing efficiency. To address these challenges, the frequency of the highest amplitude harmonic was used if its amplitude was greater than the amplitude of the stimulation frequency itself. Along with the emergence of the harmonics, we were able to show in our study that even with stimulation bellow the endogenous range, optogenetic targeting of the PV+ septal neurons was effective in superseding the endogenous oscillations. This further supports the hypothesis that GABAergic neurons act as the pacemaker of theta oscillations in the hippocampus.

In their study of context-dependent hippocampal activity in spatial alternation, Ainge et al concluded that the continuous version of the alternation task did not require the hippocampus (Ainge et al., 2007). Furthermore, they showed that by introducing delays of 2s or 10s, similar to those used in our study, the performance of animals with hippocampal lesions was impaired. Interestingly, the impairment of performance on the spatial alternation task was greater in the 10s delay condition than in the 2s delay condition (Ainge et al., 2007). This can be attributed to the fact that introducing a delay increases the spatial memory burden and that the delay interrupts the continuous trajectory of the animal form one reward site to the next. In our study, we found that in the 2s delay condition none of the stimulation frequencies caused a change in the performance of the mice on the alternation task (Figure 10). This differs from the changes observed in the 10s delay condition (Figure 11). A possible explanation for this might be that the longer delay (10s) increases the dependency of the spatial alternation task on the hippocampus compared to the 2s delay condition.

Although our behavioral data at higher stimulation frequencies (10 and 12 Hz) did not reach significance for an impairment of spatial working memory with 10s delays either before (for 10 Hz) or after (for 12 Hz) correction for multiple comparisons, we can identify a clear trend in that direction. Before Holm-Bonferroni correction, a t-test comparing the performance of the mice with the 12 Hz stimulation to baseline reached significance ($p= 0.04$). This proximity to the significance threshold after correction, is therefore something that would need to be addressed by adding more animals to our study. It is possible that our results differ from those of Quirk *et al.* because of the difference in the order of the delays which could have increased the variability or resulted in a smaller effect size. For instance, the 10s delay condition is more difficult for the mice to perform. By starting a recording day with a 10s delay, it is possible that the performance is lower than if the 10s no stimulation condition had come at a later time in the recording session. The strong trend in our data suggests that by adding more animals to our study we would be able to make more reliable conclusions.

Finally, the lower frequency stimulations, particularly the 4 Hz stimulation in the 10s delay condition, suggest that the mice's performance may improve on the spatial alternation task. Given this strong trend, we will further examine this possibility by testing additional animals. A possible explanation for the reported improvement is an increase in coordination between hippocampus and prefrontal cortex. Not only does the prefrontal cortex display an endogenous 4 Hz oscillation (Fujisawa & Buzsáki, 2011) but it is also known to be engaged during spatial working memory tasks (Riley & Constantinidis, 2016). Other studies have demonstrated that cells of the medial prefrontal cortex (mPFC) involved in behavior can be phase locked to hippocampal theta oscillation (Hyman et al., 2005; Siapas et al., 2005). This suggest that the mPFC could contribute

to the processing of information relevant to the hippocampus (Hyman et al., 2005). We hypothesize that given the role of a low frequency oscillation in the prefrontal cortex, a 4 Hz stimulated oscillation in the hippocampus could allow for these two brain regions to communicate more effectively. Alternatively, reducing the hippocampal endogenous oscillation to 4 Hz could allow the prefrontal cortex to play a larger role in the decision-making aspect of the behavioral task.

Taken together, our results point to a bi-directional effect of modulating hippocampal theta oscillation. These data contribute to the understanding of the role of theta oscillations and theta-related spike timing for spatial memory. These behavioral results, combined with recordings in different cortical regions, could pave the way to a better understanding of how precise coordination of neural activity supports cognitive functions.

CHAPTER IV- CONCLUSION

We found that modulating hippocampal theta oscillations could have opposing effects on the performance of mice on a hippocampal dependent memory task. A decrease in the oscillation frequency to 4 Hz points to a possible improvement in memory, and an increase in the oscillation frequency to 12 Hz to a possible impairment in memory. Our data suggest that these changes may only be evident in the 10s delay condition a condition in which the dependency of the spatial alternation task on the hippocampus is stronger than in the 2s delay condition. Therefore, our data show that pronounced frequency changes in hippocampal theta oscillations do not cause a deficit in versions of the spatial memory task that only moderately depend on hippocampal function. Furthermore, our data also show that artificially pacing oscillations at frequencies that are at or close to 8 Hz do not cause any deficits in a hippocampus-dependent task. Although we are not yet able to make statistically significant conclusion for the 4 Hz frequency, the pattern of results allows us to conclude that a shift to lower frequencies did not cause a deficit in performance of the spatial alternation task and will perhaps result in an improvement. Furthermore, our successful use of optogenetics to entrain the hippocampal theta oscillation to fire below its endogenous range in freely moving animals paves the way for future research to utilize this technique to analyze how cells respond to these changes.

The data in this thesis were obtained in collaboration with Fu, Maylin L; Siretskiy, Rachel E; Jaramillo, Marina A; Leutgeb, Jill K; Leutgeb, Stefan. Naomie Devico Marciano was the primary author.

REFERENCES

Ainge, J. A., Van Der Meer, M. A. A., Langston, R. F., & Wood, E. R. (2007). Exploring the role of context-dependent hippocampal activity in spatial alternation behavior. *Hippocampus*, *17*(10), 988–1002. https://doi.org/10.1002/hipo.20301

Anand, K., & Dhikav, V. (2012). Hippocampus in health and disease: An overview. In *Annals of Indian Academy of Neurology* Vol. 15, Issue 4, pp. 239–246. https://doi.org/10.4103/0972-2327.104323

Andersen, P., Bliss, T. V. ., & Skrede, K. . (1971). Lamellar Organization of Hippocampal Excitatory Pathways. In *Brain Res* Vol. 13. Springer-Verlag.

Bender, F., Gorbati, M., Cadavieco, M. C., Denisova, N., Gao, X., Holman, C., Korotkova, T., & Ponomarenko, A. (2015). *ARTICLE Theta oscillations regulate the speed of locomotion via a hippocampus to lateral septum pathway*. https://doi.org/10.1038/ncomms9521

Blumberg, B. J., Flynn, S. P., Barriere, S. J., Mouchati, P. R., Scott, R. C., Holmes, G. L., & Barry, J. M. (2016). Efficacy of nonselective optogenetic control of the medial septum over hippocampal oscillations: The influence of speed and implications for cognitive enhancement. *Physiological Reports*, *4*(23). https://doi.org/10.14814/phy2.13048

Boyden, E. S., Zhang, F., Bamberg, E., Nagel, G., & Deisseroth, K. (2005). Millisecond-timescale, genetically targeted optical control of neural activity. *Nature Neuroscience*, *8*(9), 1263–1268. https://doi.org/10.1038/nn1525

Bragin, A., Jando, G., Nadasdy, Z., Hetke, J., Wise, K., & Buzsaki, G. (1995). Gamma (40-100 Hz) oscillation in the hippocampus of the behaving rat. *Journal of Neuroscience*, *15*(1 I), 47–60. https://doi.org/10.1523/jneurosci.15-01-00047.1995

Buzsáki, G, Buhl, D. L., Harris, K. D., Csicsvari, J., Czéh, B., Czéh, C., & Morozov, A. A. (2003). *Hippocampal network patterns of activity in the mouse*.

Buzsáki, G, & Draguhn, A. (2004). Neuronal oscillations in cortical networks. In *Science* Vol. 304, Issue 5679, pp. 1926–1929. https://doi.org/10.1126/science.1099745

Buzsáki, György. (1986). Hippocampal sharp waves: Their origin and significance. *Brain Research*, *398*(2), 242–252. https://doi.org/10.1016/0006-8993(86)91483-6

Buzsáki, György. (2002). Theta oscillations in the hippocampus. In *Neuron* Vol. 33, Issue 3, pp. 325–340. Cell Press. https://doi.org/10.1016/S0896-6273(02)00586-X

Buzsáki, György, & Moser, E. I. (2013). Memory, navigation and theta rhythm in the hippocampal-entorhinal system. In *Nature Neuroscience* Vol. 16, Issue 2, pp. 130–138. https://doi.org/10.1038/nn.3304

Canali, P., Sarasso, S., Rosanova, M., Casarotto, S., Sferrazza-Papa, G., Gosseries, O., Fecchio, M., Massimini, M., Mariotti, M., Cavallaro, R., Smeraldi, E., Colombo, C., & Benedetti, F. (2015). Shared reduction of oscillatory natural frequencies in bipolar disorder, major depressive disorder and schizophrenia. *Journal of Affective Disorders*, *184*, 111–115. https://doi.org/10.1016/j.jad.2015.05.043

Chenani, A., Sabariego, M., Schlesiger, M. I., Leutgeb, J. K., Leutgeb, S., & Leibold, C. (2019). Hippocampal CA1 replay becomes less prominent but more rigid without inputs from medial entorhinal cortex. *Nature Communications*, *10*(1). https://doi.org/10.1038/s41467-019-09280-0

Cole, S. R., & Voytek, B. (2016). Brain Oscillations and the Importance of Waveform Shape. *Trends in Cognitive Sciences*, *xx*. https://doi.org/10.1016/j.tics.2016.12.008

Colgin, L. L. (2016). Rhythms of the hippocampal network. In *Nature Reviews Neuroscience* Vol. 17, Issue 4, pp. 239–249. Nature Publishing Group. https://doi.org/10.1038/nrn.2016.21

Denker, M., Roux, S., Lindén, H., Diesmann, M., Riehle, A., & Grün, S. (2011). *The Local Field Potential Reflects Surplus Spike Synchrony*. Cerebral Cortex. https://www.ncbi.nlm.nih.gov/pmc/articles/PMC3209854/

Freund, T. F. (1989). GABAergic septohippocampal neurons contain parvalbumin. *Brain Research*, *478*(2), 375–381. https://doi.org/10.1016/0006-8993(89)91520-5

Freund, T. F., & Antal, M. (1988). *GABA-containing neurons in the septum control inhibitory interneurons on the hippocampus*. 170–173.

Fries, P. (2005). A mechanism for cognitive dynamics: Neuronal communication through neuronal coherence. *Trends in Cognitive Sciences*, *9*(10), 474–480. https://doi.org/10.1016/j.tics.2005.08.011

Fuhrmann, F., Justus, D., Sosulina, L., Kaneko, H., Beutel, T., Friedrichs, D., Schoch, S., Schwarz, M. K., Fuhrmann, M., & Remy, S. (2015). Locomotion, Theta Oscillations, and the Speed-Correlated Firing of Hippocampal Neurons Are Controlled by a Medial Septal Glutamatergic Circuit. *Neuron*, *86*(5), 1253–1264. https://doi.org/10.1016/j.neuron.2015.05.001

Fujisawa, S., & Buzsáki, G. (2011). A 4 Hz Oscillation Adaptively Synchronizes Prefrontal, VTA, and Hippocampal Activities. *Neuron*. https://doi.org/10.1016/j.neuron.2011.08.018

Girardeau, G., Benchenane, K., Wiener, S. I., Buzsáki, G., & Zugaro, M. B. (2009). Selective suppression of hippocampal ripples impairs spatial memory. *Nature Neuroscience*, *12*(10), 1222–1223. https://doi.org/10.1038/nn.2384

Gogolák, G., Stumpf, C., Petsche, H., & Šterc, J. (1968). The firing pattern of septal neurons and the form of the hippocampal theta wave. *Brain Research*, *7*(2), 201–207. https://doi.org/10.1016/0006-8993(68)90098-X

Gonzalez-Sulser, A., Parthier, D., Candela, A., McClure, C., Pastoll, H., Garden, D., Sürmeli, G., & Nolan, M. F. (2014). Gabaergic projections from the medial septum selectively inhibit interneurons in the medial entorhinal cortex. *Journal of Neuroscience*, *34*(50), 16739–16743. https://doi.org/10.1523/JNEUROSCI.1612-14.2014

GREEN, J. D. (1964). The Hippocampus. In *Physiological reviews* Vol. 44, pp. 561–608. https://doi.org/10.1152/physrev.1964.44.4.561

Green, J. D., & Arduinp, A. A. (1954). *Hippocampal electrical activity in arousal 1*. www.physiology.org/journal/jn

Green, J. D., Maxwell, D. S., Schindler, W. J., & Stumpf, C. (1960). Rabbit EEG "theta" rhythm: its anatomical source and relation to activity in single neurons. *Journal of Neurophysiology*, *23*(4), 403–420. https://doi.org/10.1152/jn.1960.23.4.403

Hangya, B., Borhegyi, Z., Szilágyi, N., Freund, T. F., & Varga, V. (2009). GABAergic neurons of the medial septum lead the hippocampal network during theta activity. *Journal of Neuroscience*, *29*(25), 8094–8102. https://doi.org/10.1523/JNEUROSCI.5665-08.2009

Harris, A. Z., & Gordon, J. A. (2015). Long-Range Neural Synchrony in Behavior. *Annual Review of Neuroscience*, *38*(1), 171–194. https://doi.org/10.1146/annurev-neuro-071714-034111

Hasselmo, M. E. (2005). What is the function of hippocampal theta rhythm? - Linking bahavioral data to phasic properties of field potential and unit recording data. In *Hippocampus* Vol. 15, Issue 7, pp. 936–949. https://doi.org/10.1002/hipo.20116

Herreras, O. (2016). Local field potentials: Myths and misunderstandings. *Frontiers in Neural Circuits*, *10*(DEC). https://doi.org/10.3389/fncir.2016.00101

Hyman, J. M., Zilli, E. A., Paley, A. M., & Hasselmo, M. E. (2005). Medial prefrontal cortex cells show dynamic modulation with the hippocampal theta rhythm dependent on behavior. *Hippocampus*, *15*(6), 739–749. https://doi.org/10.1002/hipo.20106

Jacobs, J. (2014). Hippocampal theta oscillations are slower in humans than in rodents: Implications for models of spatial navigation and memory. In *Philosophical Transactions of the Royal Society B: Biological Sciences* Vol. 369, Issue 1635. Royal Society. https://doi.org/10.1098/rstb.2013.0304

Jiang, X., Gonzalez-Martinez, J., & Halgren, E. (2019). Coordination of Human Hippocampal Sharpwave Ripples during NREM Sleep with Cortical Theta Bursts, Spindles, Downstates, and Upstates. *The Journal of Neuroscience : The Official Journal of the Society for Neuroscience*, *39*(44), 8744–8761. https://doi.org/10.1523/JNEUROSCI.2857-18.2019

King, C., Recce, M., & O'Keefe, J. (1998). The rhythmicity of cells of the medial septum/diagonal band of Broca in the awake freely moving rat: relationships with behaviour and hippocampal theta. *European Journal of Neuroscience*, *10*(2), 464–477. https://doi.org/10.1046/j.1460-9568.1998.00026.x

Korte, M., & Schmitz, D. (2016). Cellular and System Biology of Memory: Timing, Molecules, and Beyond. *Physiological Reviews*, *96*(2), 647–693. https://doi.org/10.1152/physrev.00010.2015

Kramis, R., Vanderwolf, C. H., & Bland, B. H. (1975). Two types of hippocampal rhythmical slow activity in both the rabbit and the rat: Relations to behavior and effects of atropine, diethyl ether, urethane, and pentobarbital. *Experimental Neurology*, *49*(1), 58–85. https://doi.org/10.1016/0014-4886(75)90195-8

Lega, B. C., Jacobs, J., & Kahana, M. (2012). Human hippocampal theta oscillations and the formation of episodic memories. *Hippocampus*. https://doi.org/10.1002/hipo.20937

Leutgeb, S., & Mizumori, S. J. Y. (1999). Excitotoxic Septal Lesions Result in Spatial Memory Deficits and Altered Flexibility of Hippocampal Single-Unit Representations.

Lewis, P. R., & Shute, C. C. D. (1967). The cholinergic limbic system: projections to hippocampal formation, medial cortex, nuclei of the ascending cholinergic reticular system, and the subfornical organ and supra-optic crest. https://doi.org/10.1093/brain/90.3.521

Mcfarland, W. L., Teitelbaum, H., & Hedges, E. K. (1975). Relationship between hippocampal theta activity and running speed in the rat. *Journal of Comparative and Physiological Psychology*, *88*(1), 324–328.

McNaughton, N., Ruan, M., & Woodnorth, M. A. (2006). Restoring theta-like rythmicity in rats restores initial learning in the Morris water maze. *Hippocampus*, *16*(12), 1102–1110. https://doi.org/10.1002/hipo.20235

Mishkin, M. (1978). Memory in monkeys severely impaired by combined but not by separate removal of amygdala and hippocampus. *Nature*, *273*(5660), 297–298. https://doi.org/10.1038/273297a0

Montez, T., Poil, S. S., Jones, B. F., Manshanden, I., Verbunt, J. P. A., Van Dijk, B. W., Brussaard, A. B., Van Ooyen, A., Stam, C. J., Scheltens, P., & Linkenkaer-Hansen, K. (2009). Altered temporal correlations in parietal alpha and prefrontal theta oscillations in early-stage Alzheimer disease. *Proceedings of the National Academy of Sciences of the United States of America*, *106*(5), 1614–1619. https://doi.org/10.1073/pnas.0811699106

Nádasdy, Z., Hirase, H., Czurkó, A., Csicsvari, J., & Buzsáki, G. (1999). Replay and time compression of recurring spike sequences in the hippocampus. *Journal of Neuroscience*, *19*(21), 9497–9507. https://doi.org/10.1523/jneurosci.19-21-09497.1999

O'Keefe, J., & Recce, M. L. (1993). Phase relationship between hippocampal place units and the EEG theta rhythm. *Hippocampus*, *3*(3), 317–330. https://doi.org/10.1002/hipo.450030307

Ólafsdóttir, H. F., Bush, D., & Barry, C. (2018). The Role of Hippocampal Replay in Memory and Planning. In *Current Biology* Vol. 28, Issue 1, pp. R37–R50. Cell Press. https://doi.org/10.1016/j.cub.2017.10.073

Penfield, W., & Milner, B. (1958). Memory Deficit Produced by Bilateral Lesions in the Hippocampal Zone. *Archives of Neurology And Psychiatry*, *79*(5), 475–497. https://doi.org/10.1001/archneurpsyc.1958.02340050003001

Petsche, H., Stumpf, C., & Gogolak, G. (1962). The significance of the rabbit's septum as a relay station between the midbrain and the hippocampus I. The control of hippocampus arousal activity by the septum cells. *Electroencephalography and Clinical Neurophysiology*. https://doi.org/10.1016/0013-4694(62)90030-5

Quirk, C., Wright, M. K., Parsey SF, De Gruia, G. F., Leutgeb, J. K., & Leutgeb, S. (2016). *Optogenetic stimulation of parvalbumin neurons in the medial septum paces theta frequency and disrupts spatial memory* V.639 p12. Society for Neuroscience.

Rawlins, J. N. P., Feldon, J., & Gray, J. A. (1979). Septo-hippocampal connections and the hippocampal theta rhythm. *Experimental Brain Research*, *37*(1), 49–63. https://doi.org/10.1007/BF01474253

Riley, M. R., & Constantinidis, C. (2016). Role of prefrontal persistent activity in working memory. In *Frontiers in Systems Neuroscience* Vol. 9, Issue JAN2016, p. 181. Frontiers Research Foundation. https://doi.org/10.3389/fnsys.2015.00181

Robinson, J., Manseau, F., Ducharme, G., Amilhon, B., Vigneault, E., El Mestikawy, S., & Williams, S. (2016). Optogenetic activation of septal glutamatergic neurons drive hippocampal theta rhythms. *Journal of Neuroscience*, *36*(10), 3016–3023. https://doi.org/10.1523/JNEUROSCI.2141-15.2016

Shirvalkar, P. R., Rapp, P. R., & Shapiro, M. L. (2010). Bidirectional changes to hippocampal theta-gamma comodulation predict memory for recent spatial episodes. *Proceedings of the National Academy of Sciences of the United States of America*, *107*(15), 7054–7059. https://doi.org/10.1073/pnas.0911184107

Siapas, A. G., Lubenov, E. V., & Wilson, M. A. (2005). Prefrontal phase locking to hippocampal theta oscillations. *Neuron*, *46*(1), 141–151. https://doi.org/10.1016/j.neuron.2005.02.028

Squire, L. R. (2009). The Legacy of Patient H.M. for Neuroscience. In *Neuron* Vol. 61, Issue 1, pp. 6–9. https://doi.org/10.1016/j.neuron.2008.12.023

Squire, L. R., Stark, C. E. L., & Clark, R. E. (2004). The Medial Temporal Lobe. *Annual Review of Neuroscience*, *27*(1), 279–306. https://doi.org/10.1146/annurev.neuro.27.070203.144130

Stewart, M., & Fox, S. E. (1991). Hippocampal theta activity in monkeys. *Brain Research*, *538*(1), 59–63. https://doi.org/10.1016/0006-8993(91)90376-7

Vandecasteele, M., Varga, V., Berényi, A., Papp, E., Barthó, P., Venance, L., Freund, T. F., & Buzsáki, G. (2014). Optogenetic activation of septal cholinergic neurons suppresses sharp wave ripples and enhances theta oscillations in the hippocampus. *Proceedings of the National Academy of Sciences of the United States of America*, *111*(37), 13535–13540. https://doi.org/10.1073/pnas.1411233111

Vanderwolf, C. H. (1969). Hippocampal electrical activity and voluntary movement in the rat. *Electroencephalography and Clinical Neurophysiology*, *26*(4), 407–418. https://doi.org/10.1016/0013-4694(69)90092-3

Winson, J. (1978). Loss of hippocampal theta rhythm results in spatial memory deficit in the rat. *Science*, *201*(4351), 160–163. https://doi.org/10.1126/science.663646

Yoder, R. M., & Pang, K. C. H. (2005). Involvement of GABAergic and cholinergic medial septal neurons in hippocampal theta rhythm. *Hippocampus*, *15*(3), 381–392. https://doi.org/10.1002/hipo.20062

Zutshi, I., Brandon, M. P., Fu, M. L., Donegan, M. L., Leutgeb, J. K., & Leutgeb, S. (2018). Hippocampal Neural Circuits Respond to Optogenetic Pacing of Theta Frequencies by Generating Accelerated Oscillation Frequencies. *Current Biology*, *28*(8), 1179-1188.e3. https://doi.org/10.1016/j.cub.2018.02.061